ANGULAR DEPENDENCE OF THE MATRIXX EVOLUTION

Angular Dependence of the MatriXX Evolution

By DANIEL SOPHER, BMedPhys.

A thesis submitted to the School of Graduate Studies in partial fulfillment of the requirements for the degree Master of Science

McMaster University Master of Science, (2012) Hamilton, Ontario (Medical Physics)

TITLE: Angular Dependence of the MatriXX Evolution

AUTHOR: Daniel Sopher, BMedPhys

SUPERVISOR: Dr Orest Ostapiak

NUMBER OF PAGES: xiv, 63

Keywords: - IMRT, VMAT, MatriXX Evolution, Angular Response, Gantry Angle Dependent Correction Factors.

ABSTRACT

The purpose of this thesis is to explore the angular response to dose of the MatriXX Evolution, manufactured by IBA Dosimetry, a 2-dimensional ion chamber array used for patient specific quality assurance of advanced radiotherapy techniques such as IMRT and VMAT. Investigations were made to characterize the angular response of the MatriXX and describe any differences from the Philips Pinnacle^3 Treatment Planning System (TPS) used at the Juravinski Cancer Centre.

A comparison was made between the gantry angle dependent correction factors supplied by the manufacturer and those derived by measurement. Gantry angle dependent correction factors were derived, with the MatriXX under 5cm polystyrene build-up and without any build-up, for the 5 x 5 cm^2, 10 x 10 cm^2 and 20 x 20 cm^2 field sizes.

For gantry angles ranging from 320° to 40° the maximum difference between the derived gantry angle dependent correction factors and those provided by the manufacturer is 1.5%, at a gantry angle of 320°, a 5 x 5 cm^2 field and

without build-up. The differences for the 10 x 10 cm^2 and 20 x 20 cm^2 fields within this gantry angle range are less than 1%. Between gantry angles of 50° and 130° the largest difference is 4.9% at 100°, for the 5 x 5 cm^2field without build-up. The other field sizes show similar differences; 4.7% at gantry angle of 120° for 10 x 10 cm^2 with build-up and 4.0% at a gantry angle of 80° without build-up. Between gantry angles of 140° to 220° the greatest discrepancy is for the 5 x 5 cm^2 field with build-up, a difference of 3.0%. The 10 x 10 cm^2 has a maximum difference of 2.4% at gantry angles of 180° and 200°, both when the MatriXX has build-up. The maximum discrepancy for gantry angle dependent correction factors for the 20 x 20 cm^2 fields is at a gantry angle of 140°, when the MatriXX has build-up. Between the gantry angles of 230° to 310° the largest discrepancy occurs between the derived gantry angle dependent correction factors and those supplied by the manufacturer. For the 5 x 5 cm^2, 10 x 10 cm^2 and 20 x 20 cm^2 fields respectively the largest differences are 5.9%, 4.5% and 4.9%. All three occur when there is no build-up.

ACKNOWLEDGMENTS

With thanks to the members of my supervisory committee Dr Orest Ostapiak, Dr Kevin Diamond and Dr Tom Farrell; to my co-workers at the Juravinski Cancer Centre; and a special thanks to my wife, Robin.

CCCS = Collapsed Cone Convolution Superposition

dMLC = dynamic MultiLeaf Collimator

IMAT = Intensity Modulated Arc Therapy

IMRT = Intensity Modulated Radiation Therapy

SSD = Source to Surface Distance

TPS = Treatment Planning System

VMAT = Volumetric Modulated Arc Therapy

Contents

List of illustrations, charts and diagrams

List of Tables

1. Introduction

Recent developments in radiation therapy (e.g. Intensity Modulated Radiation Therapy (IMRT) and Volumetric Modulated Arc Therapy (VMAT)) have resulted in treatments that require patient-specific quality assurance due to their complexity. These treatments use the modern Linear accelerators' capabilities to adjust many different parameters accurately and simultaneously. These include using the dynamic Multi Leaf Collimator and dose rate.

One device designed to perform patient-specific quality assurance is the MatriXX Evolution, produced by IBA Dosimetry. The MatriXX is a 2-dimensional array of ion chambers.

When measurements are made for irradiations at gantry angles other than those corresponding to normal incidence on the MatriXX, the dose reported by the MatriXX does not always match that calculated by the Treatment Planning System (TPS).

In this work the angular response of the MatriXX is characterized by comparing the measured dose to that calculated using the TPS model. The angular response will be tested further in order to compare the responses of the MatriXX and TPS to build-up and field size.

Models of the MatriXX are created within the TPS to attempt to recreate the MatriXX angular response.

The manufacturer provides gantry angle dependent correction factors (henceforth referred to as correction factors) that are used to correct for the angular dependent response of the MatriXX. The correction factors are given for the range from 0° to 180° in increments of 10°, except between 85° and 95°, where the increment between each gantry angle is 1°.

The correction factors provided by the manufacturer are compared with those derived from the MatriXX measurements and TPS calculations. This is done for different field sizes and amounts of build-up. The correction factors for beams equiangular from the vertical axis are compared. The effect of couch rotation on gantry angle factor is explored. An investigation is made of the suitability of the correction factors for MatriXX pixels away from the central axis position.

2. Literature Review

With Intensity Modulated Radiation Therapy (IMRT), high dose isodose lines may be conformed to encompass an irregularly shaped target volume or avoid an organ at risk. This degree of dose shaping would be prohibitively difficult using a conformal radiotherapy technique. IMRT is delivered using the dynamic Multileaf Collimator (dMLC), available on most modern linear accelerators, to shape the incident photon fluence at a set number of gantry angles. The number of beams, and the degree of modulation in each beam, determines the complexity of the dose profiles that can be produced by the machine (Bortfeld T. , 2010). Thus a homogenous dose distribution covering target structures while avoiding organs at risk may be designed using beams of inhomogeneous intensity. This design is achieved using optimization functions to score criteria required for tumour dose distribution (Hope, Laurie, & Hanlan, 1967). Treatment planning computers use inverse planning, based on the optimization functions, to determine the optimized distribution of incident photon intensities in each beam in order to give the required distribution to the tumour target volume (Bortfeld T. , 1999)(Burman, et al., 1997).

Intensity Modulated Arc Therapy (IMAT) combines arc therapy and IMRT so that the dMLC shape the incident photon fluence intensity as the gantry rotates around the patient in a series of arcs. Multiple arcs are utilized in order to

produce greater dose conformity (Yu, 1995)(Tang, Earl, & Yu, 2009)(Shepard, Cao, Afghan, & Earl, 2007).

Volumetric Modulated Arc Therapy (VMAT) was developed to increase patient throughput while utilizing the benefits of dose optimization given by IMRT treatments. The optimization method differs from IMRT by defining the MLC aperture shapes and then using MLC leaf positions and MU weights as optimization parameters (Otto, 2008). In a VMAT treatment MLC leaves, dose rate and gantry speed are varied concurrently as the gantry undergoes a single arc of up to 360° (Otto, 2008)(Shepard, Cao, Afghan, & Earl, 2007)(Bzdusek, Friberger, Eriksson, Hårdemark, Robinson, & Kaus, 2009). During the course of a VMAT treatment the beam may need to pass through the couch. The effect of this should be considered during planning (Vanetti, Nicolini, Clivio, Fogliata, & Cozzi, 2009) (Mihaylov, Bzdusek, & Klaus, 2011).

Due to the high number of dynamic parameters within a VMAT treatment patient-specific quality assurance is needed. This may be done through various approaches: examine the log files for gantry angle, dose rate and MLC leaf position; measure using Radiochromic film or the Electronic Portal Imaging Device (EPID) (Schreibmann, Dhabaan, Elder, & Fox, 2009)(Buckey, Stathakis, & Papanikolaou, 2010).

Another method of performing patient-specific quality assurance for VMAT treatments (or IMRT and IMAT) is to use a 2-dimensional detector array.

Previous investigations into 2-dimensional ion chamber arrays have shown that it is possible to achieve a constant sensitivity within 0.5% and a dose and dose rate to water signal linearity that is good over a range of 0.1-10Gy. Tissue Maximum Ratios (TMR), output factors and beam profiles agree with Farmer Chamber measurements to within 0.5%(Amerio, et al., 2004). The short-term reproducibility was found to be less than 0.2% over the short term and the mid and long term reproducibility to be less than 1.0%, over a range of 2 to 500 MU(E. Spezi, 2005).

Investigators have evaluated diode arrays (e.g. MapCheck) and ionization chamber arrays (e.g. Im'RT MatriXX); these arrays may be mounted on the Gantry head or left on the treatment couch. They were found to be acceptable tools for 2-dimensional dose verification (Li, Yan, & Liu, 2009)(Herzen, et al., 2007)(Korevaar, Wauben, Hulst, Langendijk, & Veld, 2011).

A strong dependence of response of the MatriXX array on photon beam angle of incidence has been reported (Han, Ng, Bhagwat, Lyatskaya, & Zygmanski, 2010) (Wolfsberger, Wagar, Nitsch, Bhagwat, & Zygmanski, 2010). When comparing MatriXX measurements with those taken in a phantom that had the same geometry, but a uniform internal structure, the posterior and anterior responses differed by up to 11%. This difference is attributed primarily to a high Atomic Number (Z) material within the MatriXX. The difference could not be accounted for by uncertainty in water equivalent thickness or inhomogeneities

within the MatriXX, for the posterior irradiation geometry. The variability in the 91° – 110° range and the 260° – 269° range was ascribed to the effective path length (Wolfsberger, Wagar, Nitsch, Bhagwat, & Zygmanski, 2010).

A study of MatriXX response to peripheral dose for IMRT and VMAT irradiations using the MatriXX has been reported. Comparisons of MatriXX measurements with those recorded using a cylindrical ion chamber were made under a variety of conditions meant to simulate an IMRT treatment and a VMAT treatment. Clinical IMRT and VMAT plans were also used for the comparison. An over-response of the MatriXX to dose in the peripheral regions required a correction of about 2.0%. The over-response was attributed to lower energy scattered radiation and the Z^3 dependent photoelectric effect (Han, Ng, Bhagwat, Lyatskaya, & Zygmanski, 2010).

The angular dependence of the off axis detectors of the MatriXX has also been investigated. (Shimohigasi, et al., 2012)(Wolfsberger, Wagar, Nitsch, Bhagwat, & Zygmanski, 2010). Off axis correction factors have been found to differ from central axis correction factors by up to 7%. Using off-axis correction factors improved the passing rate between TPS calculated and MatriXX dose distributions (Shimohigasi, et al., 2012).

3. Materials

The linear accelerator used is a Varian Trilogy, capable of delivering 6 and 10 MV photons. The Varian Trilogy offers many different treatment modes besides conventional radiation therapy including IMRT and VMAT, which Varian refers to as RapidArc®(Varian Medical Systems Inc, 2012)(Webb & McQuaid, 2009). The Trilogy has an Exact® IGRT couch which is a rigid, carbon fibre shell (Varian Medical Systems Inc, 2012). The Juravinski Cancer Centre currently uses 6MV for RapidArc® treatments.

The MatriXX Evolution system, produced by IBA Dosimetry, is designed to measure rotational therapy treatments such as TomoTherapy®, Varian's RapidArc® or Elekta's VMAT. The measurement device consists of 1020 vented pixel ionization chambers placed in a 24.4 x 24.4 cm^2 plane. The separation between each chamber is 7.62 mm (IBA Dosimetry, 2012). The MatriXX uses OmniPro-I'mRT Software(OmniPro-I'mRT Software, 2012). The MatriXX system comes with a Gantry Angle Sensor (GAS) and with correction factors that compensate for non-uniform angular dependence of the ion chambers (IBA Dosimetry, 2012).

The Philips Pinnacle^3 TPS was used to calculate expected doses to the MatriXX. The Pinnacle TPS uses Collapsed Cone Convolution Superposition (CCCS) in order to calculate dose distributions (Koninklijke Philips Electronics N.V., 2012). A CT image set of the MatriXX was acquired using a GE CT

Scanner. Varian has supplied a couch model for the IGRT couch, which has an outer shell of density 0.35g/cm^3 surrounding an air equivalent section (i.e. a density of 0g/cmm^3). This couch model was imported into the Pinnacle plans to account for the presence of the couch. For right-side up irradiations of the MatriXX, the couch model is placed beneath the MatriXX and any backscatter material used, while for up-side down irradiation of the MatriXX, the couch model is placed above the MatriXX and any backscatter material used.

RadCalc® is a Sun Nuclear software package used to perform independent MU or dose point verification calculations for TPS.(Sun Nuclear Corporation, 2012)

Some dose measurements were made with the Exradin miniature Shonka thimble model A1SL ion chamber. The A1SL has 6.4mm diameter and a collection volume of 0.053 cubic centimetres (Standard Imaging Inc, 2012). The electrometer used was a Fluke Advanced Therapy Dosimeter model 35040.

Standard Imaging's Stereotactic Dose Verification Phantom, known as the "Baby Blue" phantom, was used for some ion chamber measurements. The Baby Blue phantom is a 20 x 20 cm^2 layered, solid water phantom of variable thickness. It can be also used for film measurements (Standard Imaging, Inc, 2012).

4. Methods

4.1. Initial Setup

The MatriXX Evolution was placed on Varian's Exact® IGRT couch, with the Source to Surface Distance (SSD) set to 99.5 cm and the centre of the MatriXX positioned on the optical crosshairs so that the machine isocentre is in the plane defined by the effective point of measurement of the ion chamber array. The MatriXX electronics were inferior to the field. Gantry angle, Collimator angle and Couch angle were all set to 0°. 4.46 cm of polystyrene build-up was placed on top of the MatriXX. The field size was 20 cm square.

Figure 1: The MatriXX evolution placed upon the Exact® IGRT couch with 5cm of build-up. The linac is a Varian Trilogy

The gantry was rotated around the MatriXX, in 10° intervals, with 100 Monitor Unit (MU) irradiations made, every interval. The photon energy for every measurement was 6 MV. The setup is shown in Figure 1.

The MatriXX calibration is performed according to the equation below:

$$D_{ij} = (M\text{-}B)_{ij} * N_D^W(60Co) * K_{uni,\,ij} * k_{pT} * K_{off,\,i,j} * k_{User}$$

Where D_{ij} = Calibrated dose

M_{ij} = Matrix of measured values

B_{ij} = Matrix of background values

$N_D^W(60Co)$ = Calibration to cobalt in Gy/nC at reference temperature and pressure

$K_{uni,\,ij}$ = Uniformity Correction Matrix

k_{pT} = correction for pressure (P) and temperature (T) = ——— —

k_{User} = Factor for the detector, obtained by the value of a dose rate or dose measurement in a reference chamber, divided by the average of the values of 4 middle chambers in MatriXX

$K_{off,\,i,j}$ = Additional off axis calibration

$K_{off,\,i,j}$ and k_{User} can both be defined by the MatriXX user.

The sensitivity of the MatriXX is generally taken to be 0.42 Gy/nC(IBA Dosimetry, 2012).

The central position of the MatriXX does not contain an ion chamber so the four surrounding ion chambers were used to find the dose average for the central position. The variation of MatriXX detectors has been previously recorded as 1.0%(Han, Ng, Bhagwat, Lyatskaya, & Zygmanski, 2010) and this was taken to be the MatriXX error.

Prior to use the MatriXX needs to be turned on for at least two hours, and given a pre-irradiation of 1000MU at a field size of 27 x 27cm^2.

Within the Pinnacle^3 TPS the dose at the isocentre was calculated for each gantry angle measured. The area of the MatriXX that contains the ion chambers was initially contoured and the density overridden with 1g/cm^3. A 30 x 30 x 4.6 cm^3 rectangular prism was contoured on top of the MatriXX to represent the build-up and assigned a density of 1 g/cm^3. The geometry of the phantom is shown in Figure 2. The dose calculated by the TPS for these standard geometries is determined from an output factor table that is directly measured. The Linac is maintained to within ± 0.5% of the calibrated dose-rate. Thus, the error for the TPS calculation is taken as ± 0.5%.

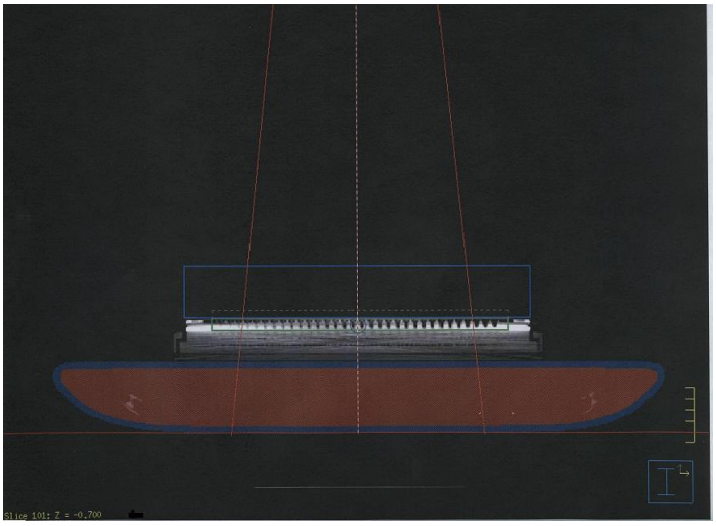

Figure 2: An image of the MatriXX as it is shown in the TPS. The couch model is provided by Varian. The contoured blue box on the anterior of the MatriXX represents the polystyrene build-up, and has had the density overridden to 1.0 g/cm^3

The effective point of measurement was varied, aling the beam axis, within the TPS to try to establish the same results as measured by the MatriXX.

TPS models with and without the unit density contour over the ion chambers were compared. The unit density contour over the ion chambers was removed for all subsequent TPS calculations.

4.2. Measuring the dose using an A1SL chamber

The MatriXX was placed in a polystyrene phantom and cantilevered off the superior side of the couch. The phantom known as the "Pelvis Phantom" is 5

cm thick from the exterior edge of the MatriXX. The anterior section of the pelvis phantom was removed and was replaced with a similar section that could hold an Exradin A1SL ion chamber at the centre position as shown in Figure 3. The A1SL chamber was flush against the MatriXX surface and beneath the polystyrene. Comparisons were made between the absolute dose measured using the ion chamber and electrometer system and the TPS at gantry angles from 0-350° in increments of 10° in order to determine the accuracy of the TPS system in calculating dose to the ion chamber's effective point of measurement for a geometry that closely parallels that of the MatriXX irradiations. All irradiations used 100 MU of 6 MV x-rays. The difference between the measured dose and the TPS calculated dose was recorded for each angle. The MatriXX density was not over-ridden in the TPS.

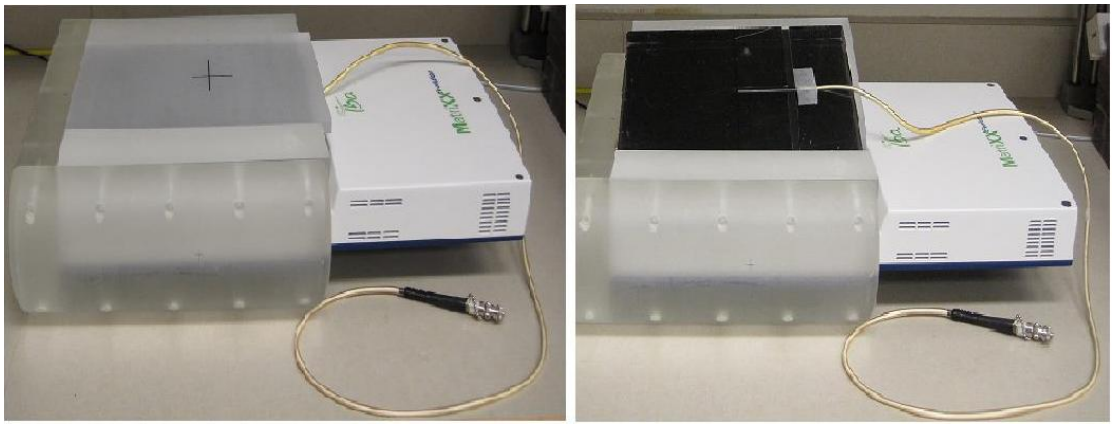

Figure 3: The MatriXX encased within the "Pelvis Phantom" with an A1SL ion chamber. The upper portion of the phantom had been removed and replaced with a section that can hold an A1SL chamber

4.3. A comparison of Tissue Phantom Ratios (TPR)

A comparison of TPR's was made between RadCalc, an ion chamber and electrometer, the TPS and the MatriXX system; in each of these systems the build-up was varied and the machine isocentre positioned with the nominal point of measurement of each dose system and irradiated with the gantry at 0°. These values were normalized to unity at 5cm of depth.

4.4. Testing the couch model using an ion chamber

In order to test the validity of the IGRT couch model used in the TPS an Exradin A1SL ion chamber, connected to an electrometer, was placed in the Standard Imaging "Baby Blue" Phantom as shown in Figure 4.

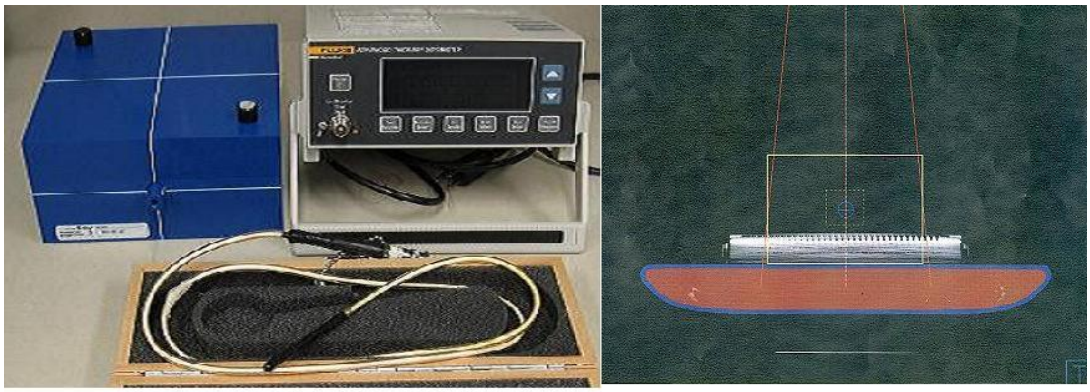

Figure 4: The "Baby Blue" phantom, A1SL chamber and electrometer, used to determine ratio of the doses at 0° and 180° and how it is represented in the TPS (Right)

The ion chamber was placed at the LINAC isocentre and irradiated with the gantry at 0° and 180°. The ratio of charge collected in these two geometries was

compared to that found using the TPS. The TPS used a virtually created cube of the same dimensions (20 x 20 x 10cm^3) and density (1.1 g/cm^3) as the solid water phantom. All irradiations used 100 MU of 6 MV x-rays.

4.5. Investigating up-side down orientated MatriXX response to depth

The MatriXX Evolution was placed upside down on the Varian's Exact® IGRT couch, with the scribed marks on either side aligned with the isocentre and the centre of the MatriXX aligned with the optical crosshairs. The scribed marks match the extent of the intrinsic build-up of the MatriXX. The MatriXX electronics were inferior to the field. Gantry angle, Collimator angle and couch angle were all set to 0°. The photon energy for every measurement made was 6 MV.

The build-up on the posterior side of the MatriXX was varied and the dose measured by the MatriXX was compared with that found using the TPS. The model was flipped so that the anterior side of the scanned MatriXX abutted the couch.

The Gantry angle was rotated to 180° and the MatriXX irradiated right side up from the posterior side, with the couch in the beam. The amount of polystyrene between the beam source and the MatriXX was varied. The dose measured by the MatriXX was compared with that found using the TPS. All irradiations were of 100 MU and photon energy of 6 MV.

4.6. Investigating MatriXX response to field size, for different build-ups with the MatriXX oriented right side up and upside down

The MatriXX was placed on the IGRT couch in the original setup and then with the MatriXX upside down. The dose was found for various field sizes (1 x 1 cm^2, 2 x 2 cm^2, 5 x 5 cm^2, 10 x 10 cm^2, 15 x 15 cm^2, 20 x 20 cm^2 and 25 x 25 cm^2) and with differing amount of polystyrene between the beam source and the MatriXX ion chambers. The build-up used for the anterior irradiation was, including the 0.5cm of intrinsic build-up, 0.5 cm, 3.25 cm, 5.0 cm and 10.0 cm. The build-up used for the posterior irradiation, including the 3.25 cm of intrinsic build-up, was 3.25 cm, 5.0 cm and 10.0 cm. All irradiations were of 100 MU and photon energy of 6 MV.

4.7. Creating a MatriXX model within the TPS to match the MatriXX results

Virtual models of the MatriXX were created within the TPS; contours were created of varying densities and shapes. Two of these virtual models (described below) will be compared with the MatriXX results. The first has a 1cm compensatory foil of 5g/cm^3 density within the MatriXX and is shown in Figure 5.

The second has two symmetrical air wedges (of density 0 g/cm^3) within the couch, which has a density of 1 g/cm^3. Compensatory rectangular prisms have been placed at the edge of the MatriXX that have a density of 2.5 g/cm^3.

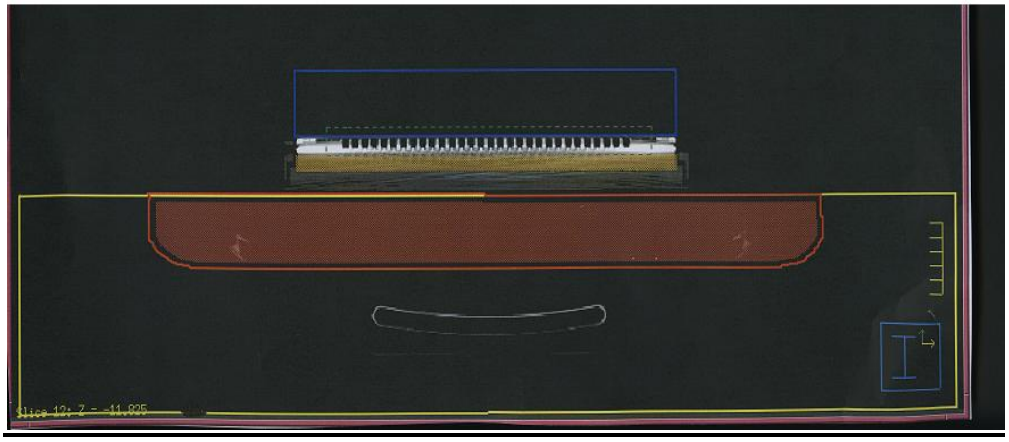

Figure 5: The "Foil" model, as shown in the TPS, used to calculate the same dose as was measured by the MatriXX. A high-density foil, in orange, was contoured within the MatriXX

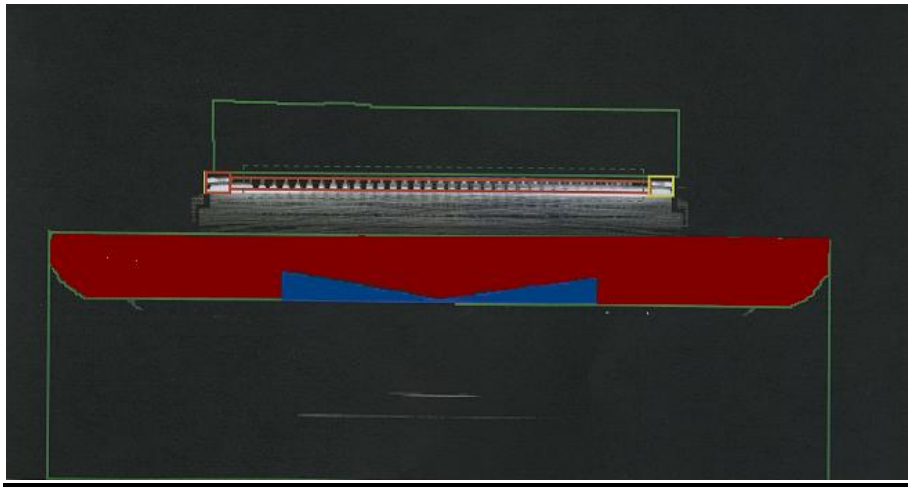

Figure 6: The "Wedge" model, as shown in the TPS, used to calculate the same dose as was measured by the MatriXX. The Varian supplied couch has been replaced with a density of 1g/cm^3 (in red) and two zero density triangles contoured, in blue. There are high-density rectangular prisms at the laterals

The ion chamber area has been contoured and given a density of 0.9 g/cm^3. The "Wedge Model" is shown in Figure 6.

4.8. Comparing the derived correction factors with those provided by IBA Dosimetry

In order to compare the Gantry Angle correction factors given by IBA, the MatriXX was cantilevered off the edge of the IGRT couch, as shown in Figure 7. The Source-Surface Distance (SSD) to the MatriXX, without any build-up, was 99.5cm. The Collimator and Couch angle were 0°. The average dose recorded by the central four chambers of the MatriXX was divided by that calculated by the TPS to determine the set of correction factors for a 20 x 20 cm^2 field at gantry angles of 0-85° in 5° increments, then from 86-95° in 1° increments, then from 100° to 180° in 5° increments and then from 180° – 350° in 10° increments.

This was repeated with a polystyrene phantom encasing the MatriXX. The phantom (known as the "Pelvis Phantom") is 5 cm thick from the exterior of the MatriXX, shown in Figure 8. The SSD was realigned to correct for any MatriXX sag. Measurements were also made for 5 x 5cm^2 and 10 x 10 cm^2 fields, with and without the phantom in place. Measurements were made for increments in gantry angle of 10° from 0-350°. All irradiations used 100 MU.

Figure 7: The MatriXX, without build-up, cantilevered of the Exact® IGRT couch

Figure 8: The MatriXX, with build-up, cantilevered off the Exact® IGRT

4.9. How the couch angle affects correction factors

The MatriXX was cantilevered off the superior edge of the Exact® IGRT as in section 4.7, but with the couch rotated 45°. Measurements were made for a

20 x 20 cm^2 field at gantry increments of 10° from 0-180°. The range of gantry angles was restricted so that the electronics of the MatriXX were not irradiated. All irradiations used 100 MU of 6 MV x-rays.

4.10. How the field position affects correction factors

With the MatriXX cantilevered off the superior end of the couch, as described in section 4.7, doses from the TPS and the MatriXX were found and used to derive correction factors at different positions within each quadrant of the field and at the centre of the field. The positions for the 20 x 20 cm^2 field are shown in Figure 9, where the green square represents the field edge and the red crosses represent the positions where the correction factors were found.

The average of the four ion chambers surrounding the position were used to find the point dose. Correction factors were found for 5 x 5 cm^2, 10 x 10 cm^2 and 20 x 20 cm^2 fields, both with and without build-up. Table 1 shows the position where correction factors were measured for each field size.

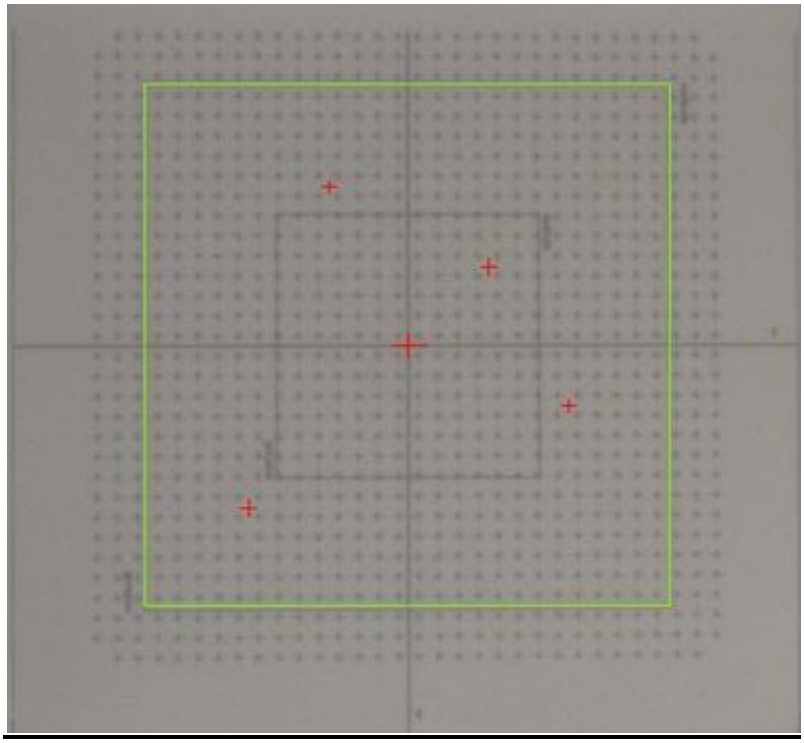

Figure 9: An image of the anterior face of the MatriXX with the green outline representing the 20 x 20cm^2 field and the red pluses (+) points where correction factors were found.

Table 1: The position where correction factors were found, for each field size

Field Size	Position 1	Position 2	Position 3	Position 4	Position 5
5 x 5 cm^2	(0,0)	(0.7,0.7)	(-0.7,1.4)	(1.4, -0.7)	(-1.4, -1.4)
10 x 10 cm^2	(0,0)	(1.4,1.4)	(-1.4,2.8)	(2.8, -1.4)	(-2.8, -2.8)
20 x 20 cm^2	(0,0)	(2.8,2.8)	(-2.8,5.6)	(5.6, -2.8)	(-5.6, -5.6)

5. Results

5.1. Initial Setup

Figure 10 shows the doses obtained from the MatriXX and those calculated using the TPS, plotted as a function of gantry angle, for measurements taken in the geometry outlined in Section 4.1.

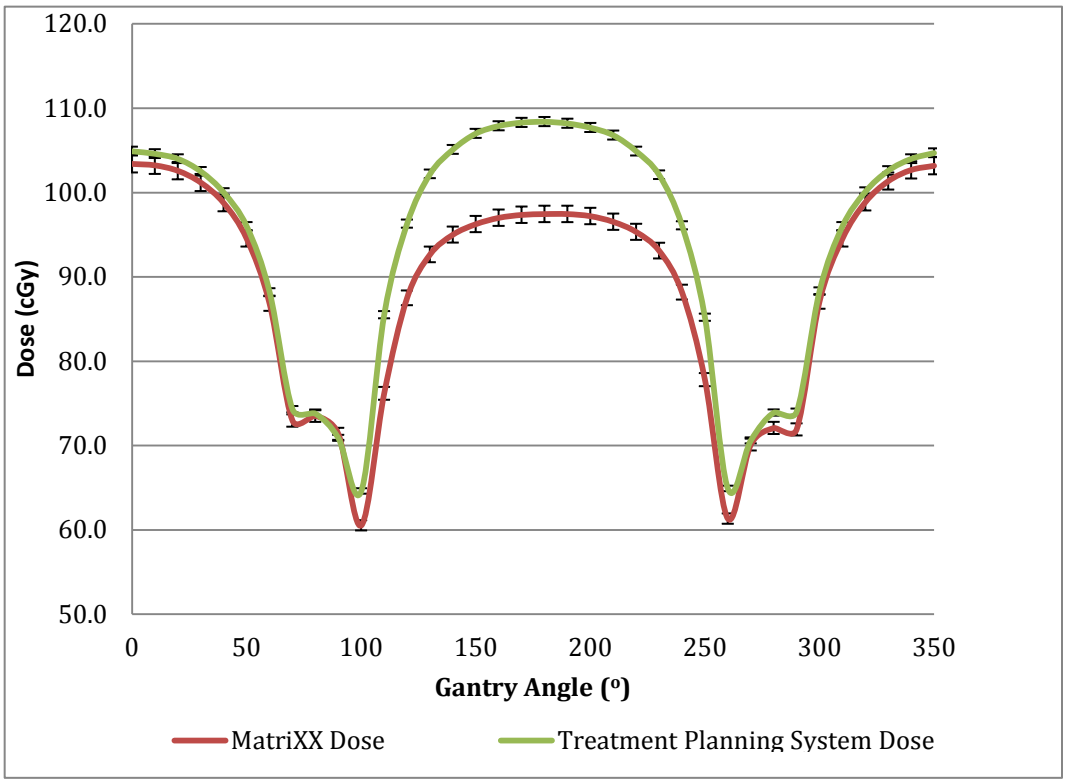

Figure 10: Dose, as a function of gantry angle, measured by the MatriXX and calculated by the TPS

Figure 11 shows the percentage difference between the doses obtained from the MatriXX and the TPS.

Figure 11: Percentage difference in dose, as a function of gantry angle, measured by the MatriXX and calculated by the TPS

Figure 12 shows the effect of moving the calculation point within the TPS's model of the MatriXX. The values at gantry angles of 0° and 180° are compared. The values found from the MatriXX have also been plotted. This shows that the point of measurement is not the cause of the discrepancy between the doses measured by the MatriXX system and those predicted by the TPS since there is no depth for which 0° and 180° incidence yield values which agree with the corresponding values determined from the TPS; even allowing for re-normalization with a simple factor.

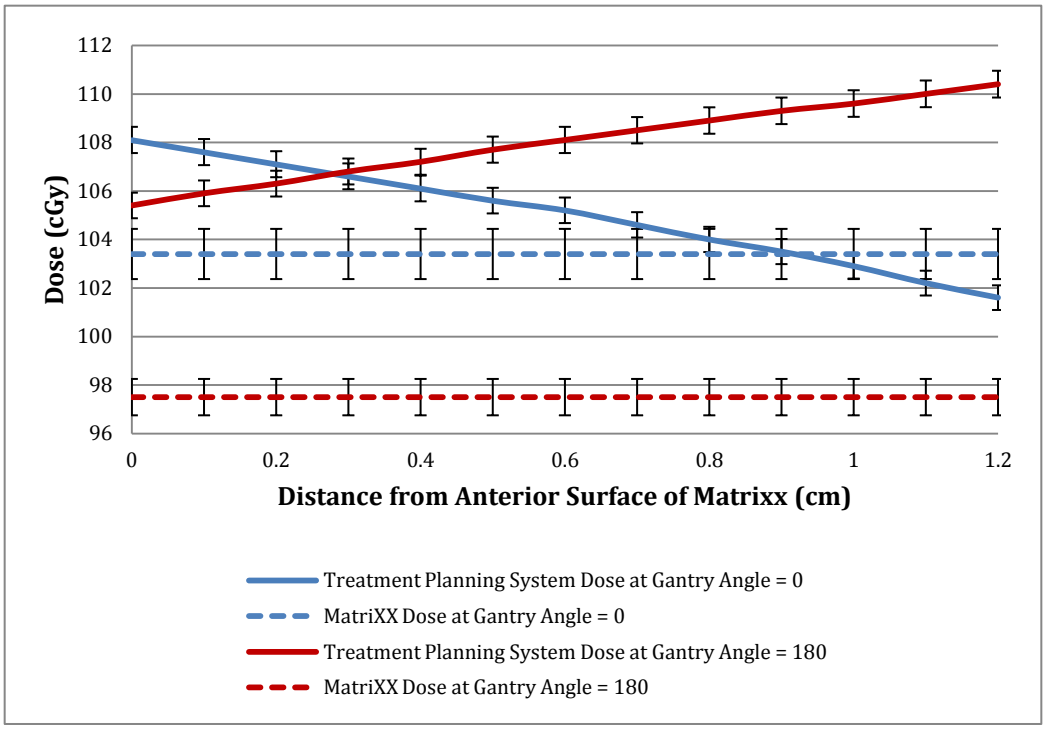

Figure 12: Modeling the effective point of measurement in the TPS. The dashed lines represent a single dose taken by the MatriXX.

Figure 13 shows that removing the contoured box of unit density from the ion chambers of the MatriXX modeled in the TPS, do not affect the dose predicted by the TPS sufficiently to explain the discrepancies between the TPS and the dose measured by the MatriXX.

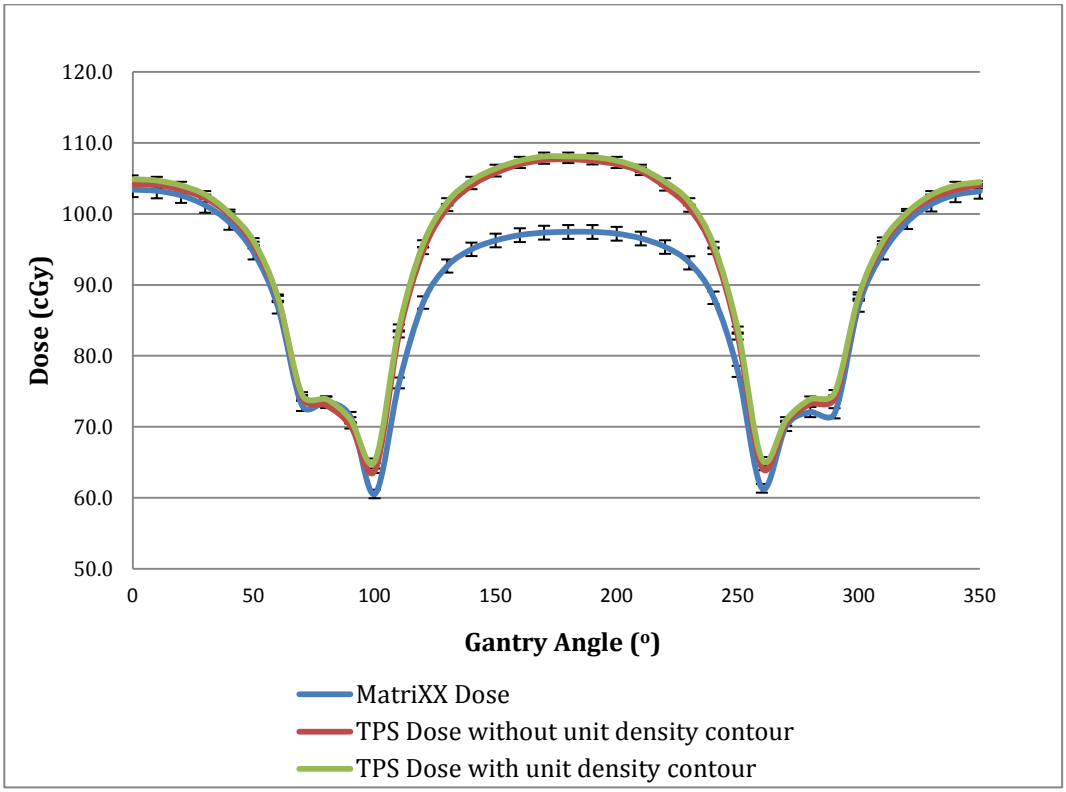

Figure 13: The effect of removing the contoured area of unit density on the TPS dose.

The contoured area covering the ion chambers of the plan of the MatriXX within the TPS was removed for the rest of the thesis unless explicitly mentioned.

5.2. Measuring the dose using an A1SL chamber

In order to calculate the dose using the A1SL ion chamber and electrometer, as described in section 4.1 and shown in Figure 3, the TG-51 protocol was followed (Almond, et al., 1999).

Where = Absorbed Dose to water at the point of measurement of the ion chamber placed under reference conditions,

M = Raw result from electrometer measured in nC,

= The correction for Temperature (T) and Pressure (P) variation

= ——— —

= The correction for ion re-combination,

= The correction for chamber polarity effects,

= The correction for electrometer inaccuracy when calibrated separately,

= The quality conversion factor to convert to a calibration factor for a beam of quality Q and

= The absorbed dose to water calibration factor as found by a national primary standard.

The average temperature over the measurements was 22.4 ± 0.2^{o} C and the pressure was 735.4 ± 0.3 mm Hg, so the correction for Temperature and Pressure was 1.035 ± 0.009. In this system the , and were all 1.00 ± 0.005, the = 1.00 ± 0.005 and the = 55.9 ± 0.6. Three measurements

were made for each raw measurement and the error corresponded to a 95% confidence interval.

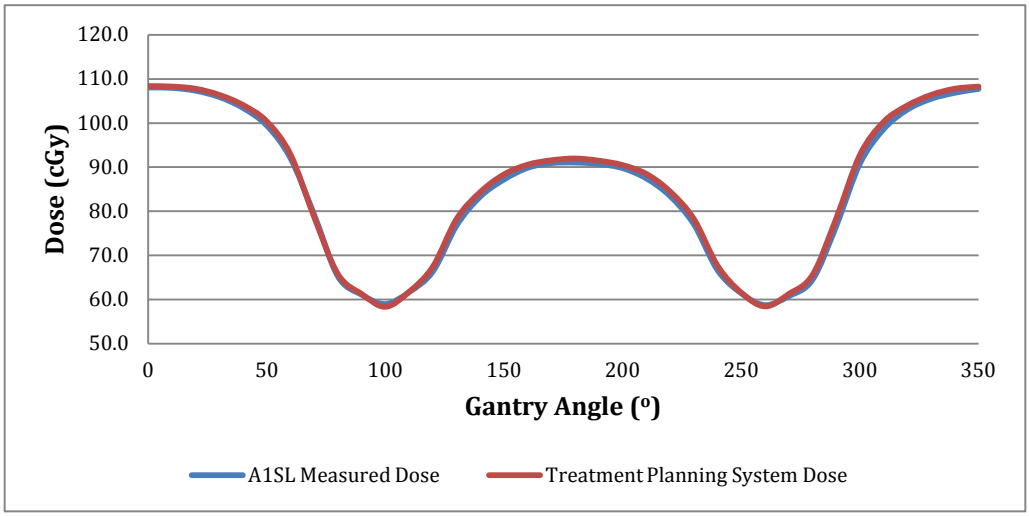

Figure 14: Dose, as a function of gantry angle, as measured by the A1SL and calculated by the TPS

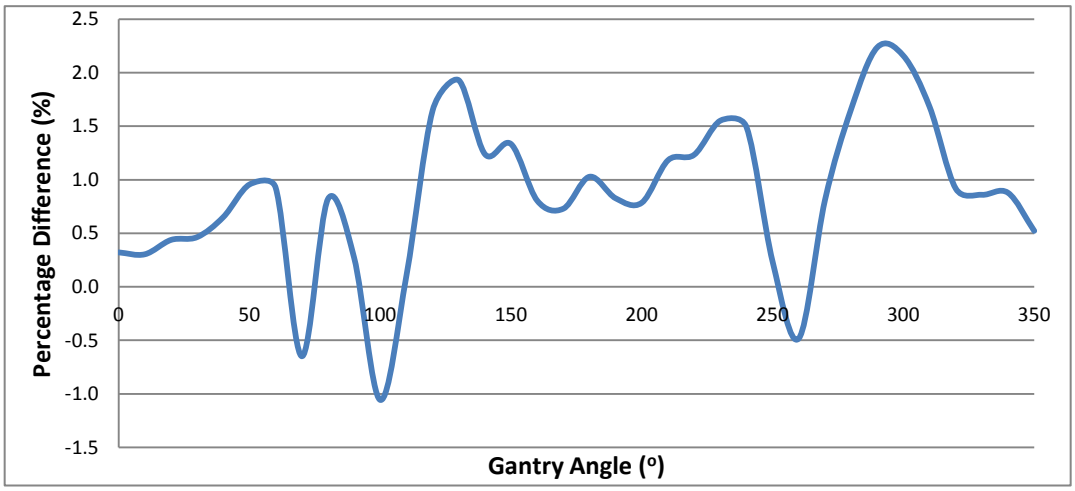

Figure 15: Percentage difference in dose, as a function of gantry angle, measured by the MatriXX and calculated by the TPS

Figure 14 shows the A1SL doses and those calculated using the TPS plotted as a function of gantry angle. The percentage difference between the two curves is shown in Figure 15.

5.3. A comparison of Tissue Phantom Ratios (TPR)

Figure 16 shows the variation of dose with build-up depth for four dosimetric systems used at the JCC: ion chamber and electrometer, RadCalc, MatriXX and Pinnacle TPS, when the gantry angle is at 0° for the geometry set out in Section 4.2. The error was taken to be 0.5% for all four systems.

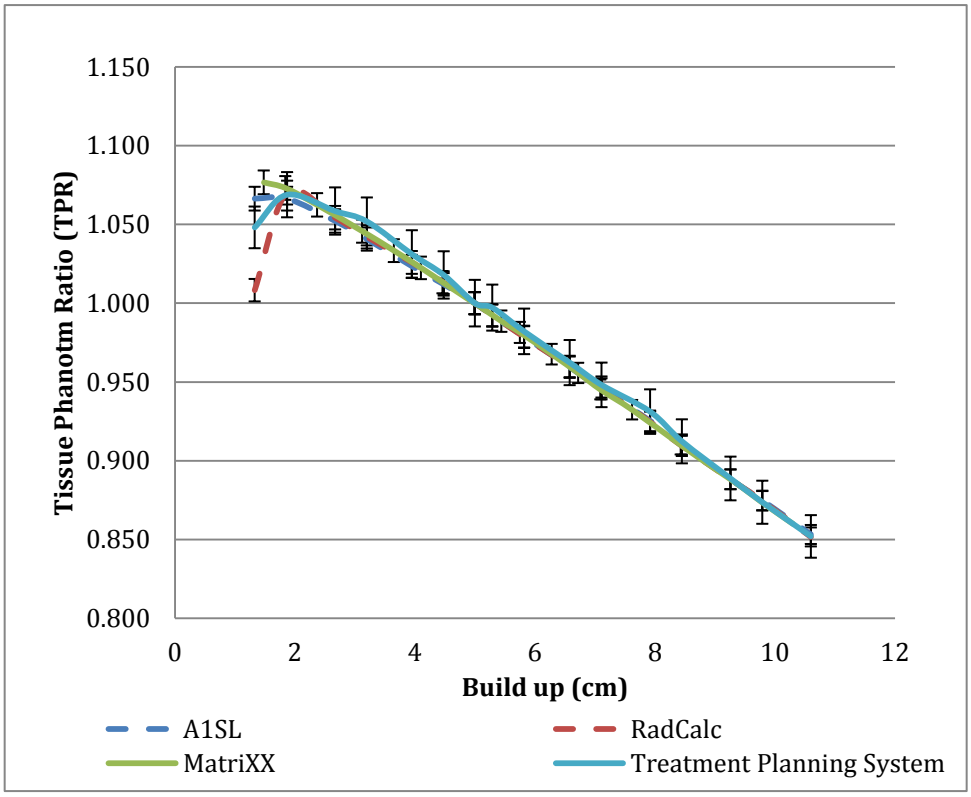

Figure 16: A comparison of normalized dose systems normalized at 5cm of depth

All the results were normalized at 5cm depth. Due to the physical size constraints of the polystyrene that held the ion chamber, measurements with less than 1.33 cm of build-up were not taken.

5.4. Testing the couch model using an ion chamber

Table 2 shows the ratio of doses determined at gantry angles of 0° and 180° using an A1SL ion chamber and electrometer and the TPS using the geometry outlined in Section 4.3

Table 2: Comparing the ratio of doses, for gantry angles of 0° and 180°, of the TPS and an A1SL ion chamber and electrometer

Readings from Ion Chamber and Electrometer (nC)					
Gantry Angle	Reading 1	Reading 2	Reading3	Average	Error
0	0.2328	0.2324	0.2327	0.2326	0.0004
180	0.2297	0.2297	0.2297	0.2297	0.00005
Ratio G_0 Reading/G_{180} Reading				1.013	0.002
Readings from Treatment Planning System (cGy)					
Gantry Angle				Average	Error
0				97.8	0.5
180				96.3	0.5
Ratio G_0 Reading/G_{180} Reading				1.016	0.007

Because the three A1SL measurements were the same at the 180° gantry angle the error was taken as half of the least significant digit or 0.00005.

5.5. Investigating up-side down orientated MatriXX response to depth

Figure 17 shows the effect of having the MatriXX up-side down, so that when the gantry angle is 0° the beam passes through the posterior side of the MatriXX as outlined in Section 4.4.

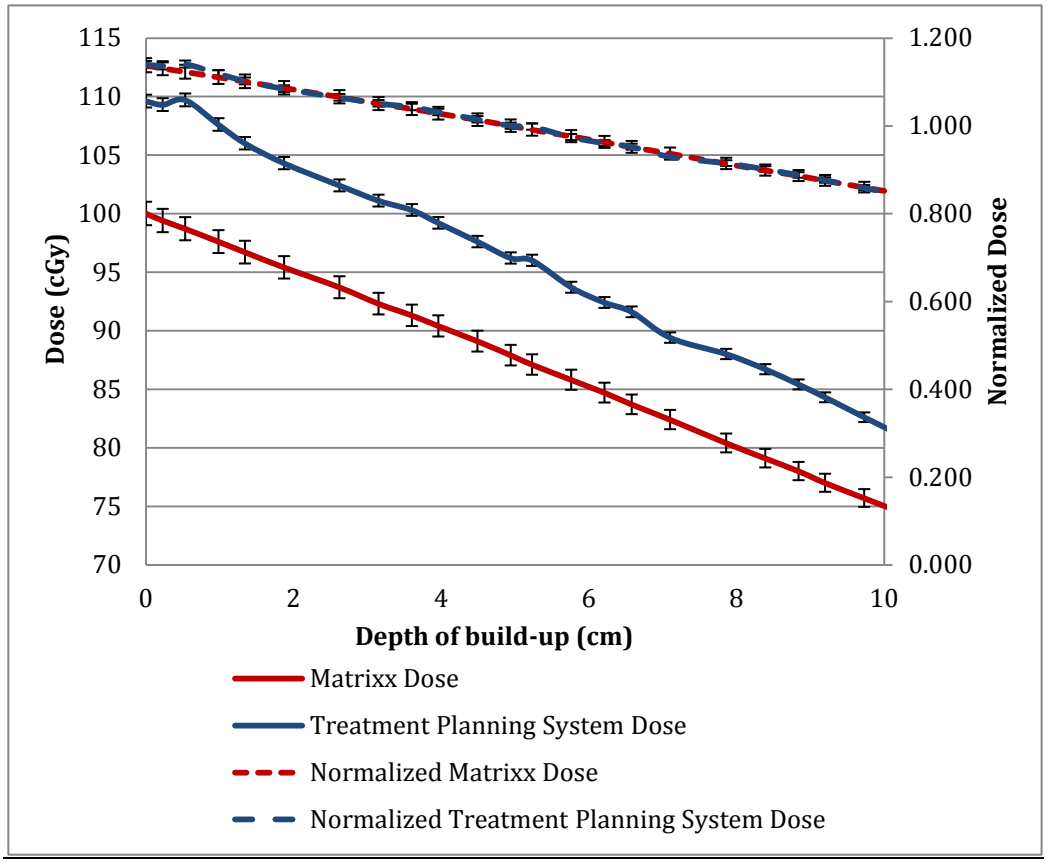

Figure 17: A comparison of the MatriXX and TPS doses measured after passing through the posterior of the MatriXX with gantry angle at 0°

The value is compared with the dose calculated by the TPS. The curves, normalized to unity at an extrinsic build-up depth of 4.9 cm, have also been plotted.

This was repeated with the Gantry at 180° and the MatriXX placed the right side up, build-up was placed between the beam source and the MatriXX. These results are shown in Figure 18. The curves, normalized to unity at a build-up depth of 5.0 cm, have also been plotted.

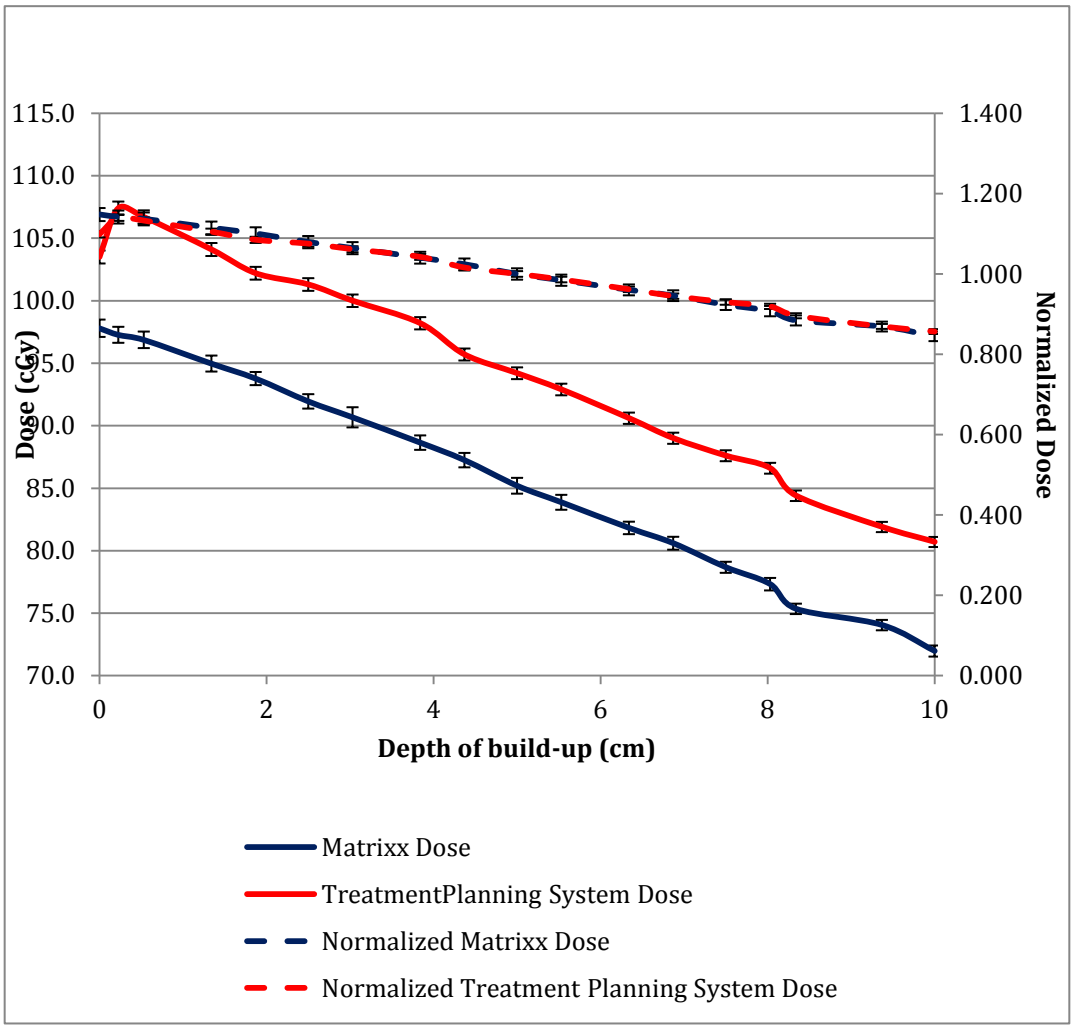

Figure 18: A comparison of the MatriXX and TPS doses measured after passing through the posterior of the MatriXX with gantry angle at 180°

5.6. Investigating MatriXX response to field size, for different build-ups with the MatriXX oriented right side up and upside down

In order to evaluate the consistency of MatriXX response with field size and depth, for right side up irradiations, the TPS calculated and MatriXX measured results are set out in Figure19, for the geometry specified in section 4.6.

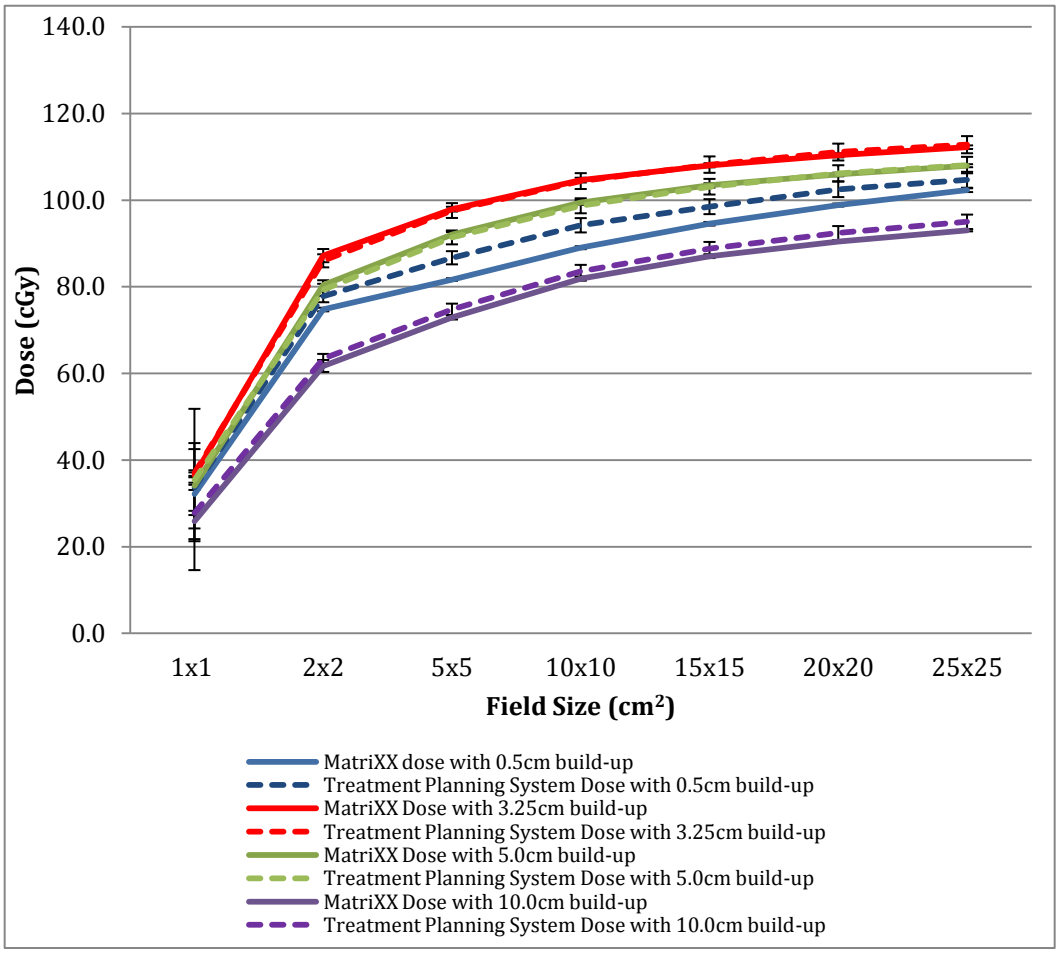

Figure 19: Calculated and measured dose as a function of field size for selected build-up depths, with the MatriXX right side up

Figure 20 shows the ratio of the calculated TPS dose to the MatriXX measured dose for the MatriXX placed right side up. Both the MatriXX and the TPS are both calibrated so that a 10x10 cm^2 field at a depth of 5cm of water is equivalent to 100cGy. The 1 x 1 cm^2 fields have been removed, as the distance between the ion chambers places the points of measurement within the penumbra.

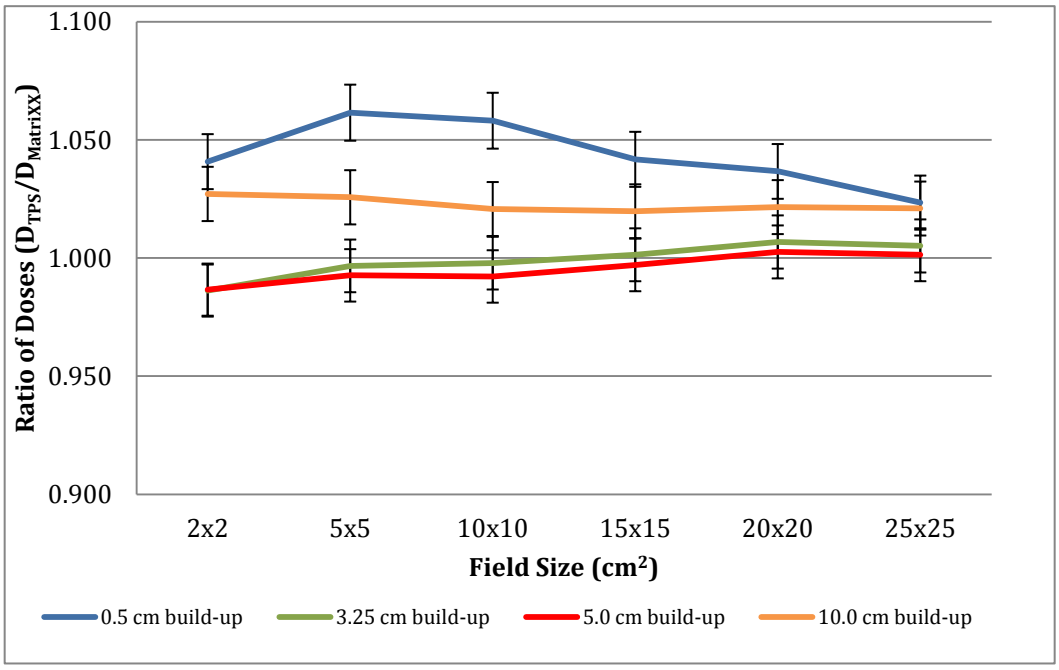

Figure 20: The ratio of calculated TPS dose to MatriXX measured dose with the MatriXX right side up.

In order to evaluate the consistency of MatriXX response with field size and depth, for upside down irradiations, the TPS calculated and MatriXX measured results, for the geometry specified in section 4.6, are set out in Figure 21.

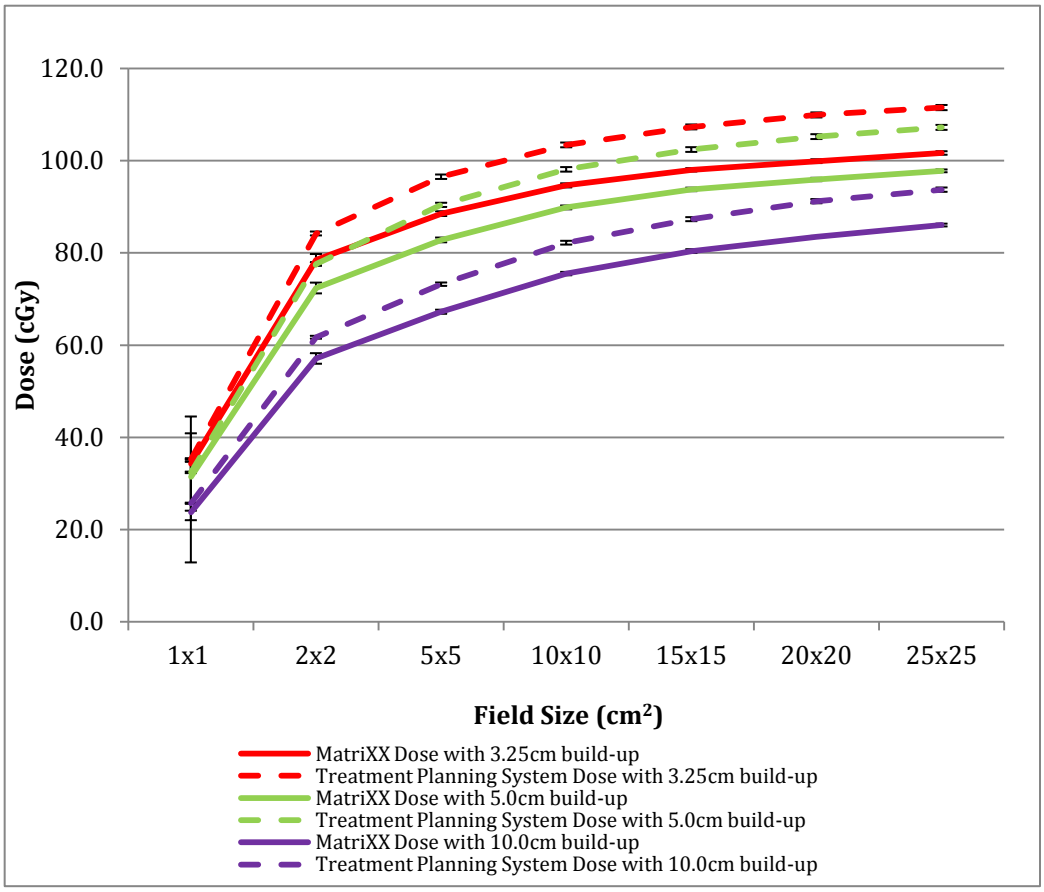

Figure 21: Calculated and measured dose as a function of field size for selected build-up depths, with the MatriXX upside down. The build-up is between the MatriXX rear and the gantry head

The ratio of the calculated TPS dose and the measured MatriXX dose, with the MatriXX positioned upside down, is shown in Figure 22.

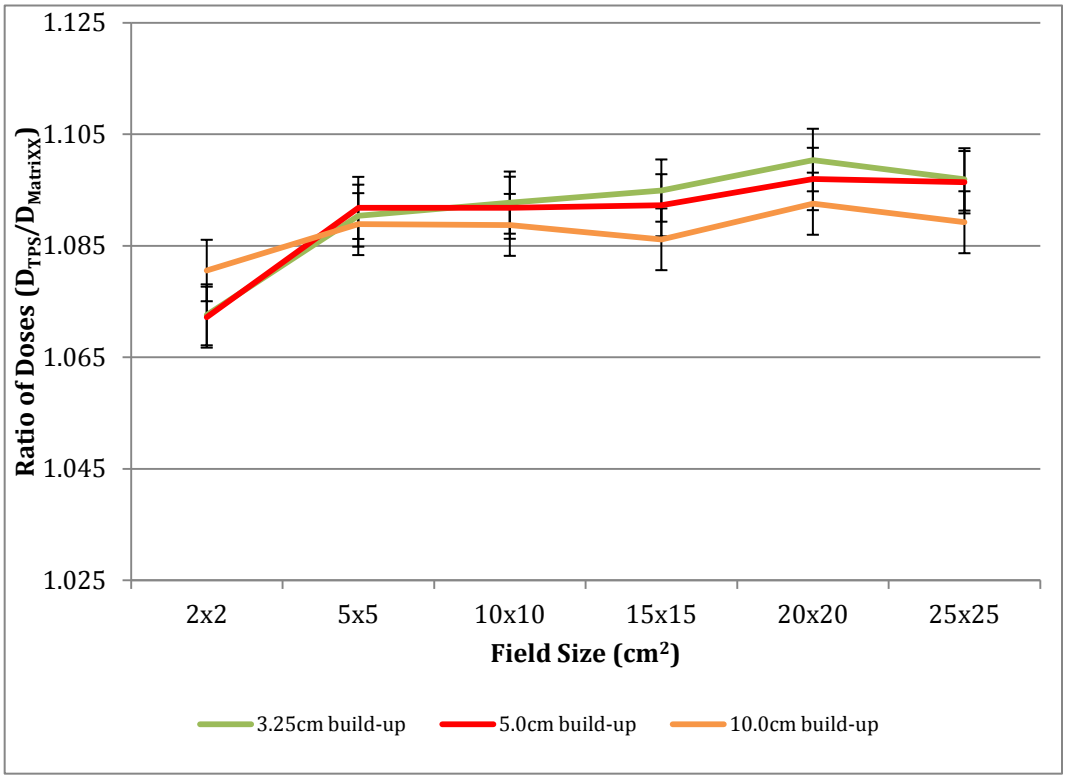

Figure 22: The ratio of calculated TPS dose to MatriXX measured dose with the MatriXX upside down

5.7. Creating a MatriXX model within the TPS to match the MatriXX results

A comparison of the two TPS models (the "Foil Model" and the "Wedge Model") and the MatriXX results are shown in Figure 23.

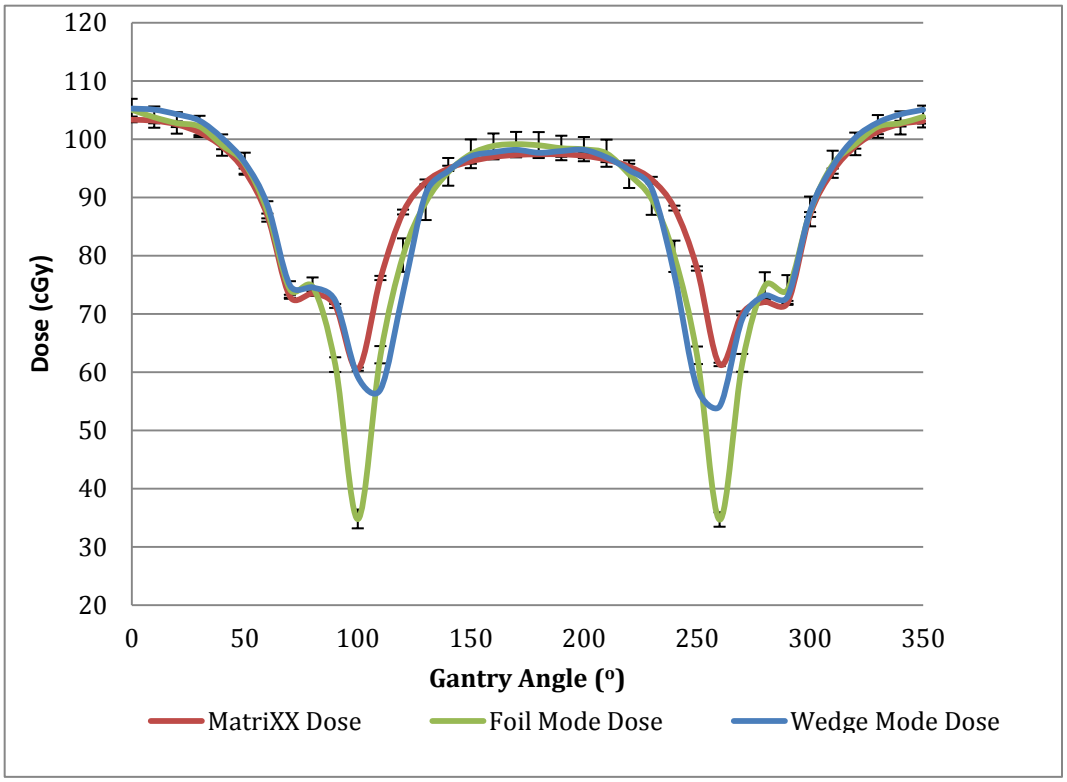

Figure 23: A comparison of TPS models designed to match the MatriXX results

5.8. Comparing the derived correction factors with those provided by IBA Dosimetry

Figure 24 is a plot of the correction factors determined using the MatriXX measurement and the TPS, both with and without build-up as described in Section 4.7. These values are compared to those given by IBA Dosimetry. The gantry angles range from 0-85° in 5° increments, from 86-95° in 1° increments and from 100-180° in 5° increments. The error associated with the factory determined correction factors is half the least significant digit or 0.0005.

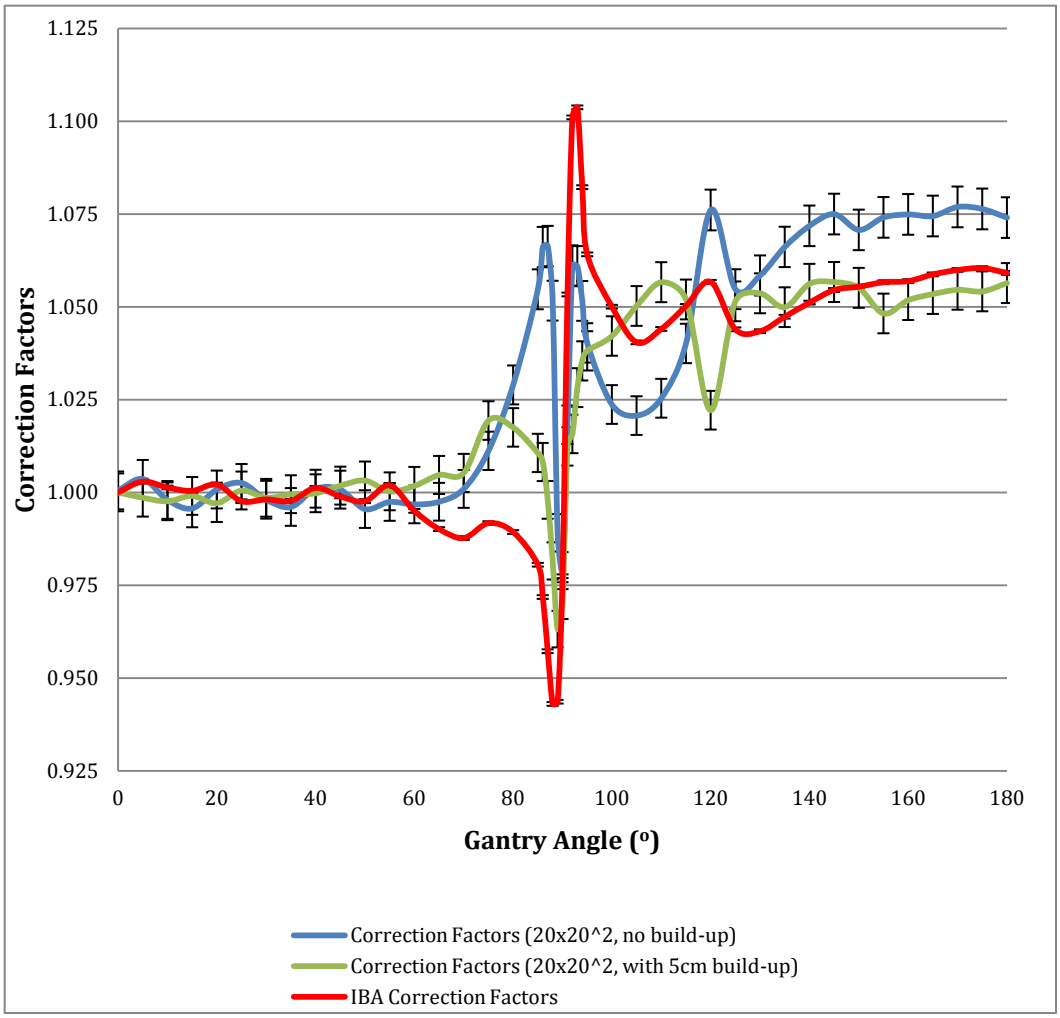

Figure 24: Derived correction factors, with and without build-up, and those provided by the manufacturer as a function of gantry angle.

The IBA Dosimetry correction factors are only given for 0-180°. Figure 25 plots the angular equivalent correction factors for 5 x 5 cm^2, 10 x 10 cm^2 and 20 x 20 cm^2 fields without build-up, and the IBA Dosimetry correction factors.

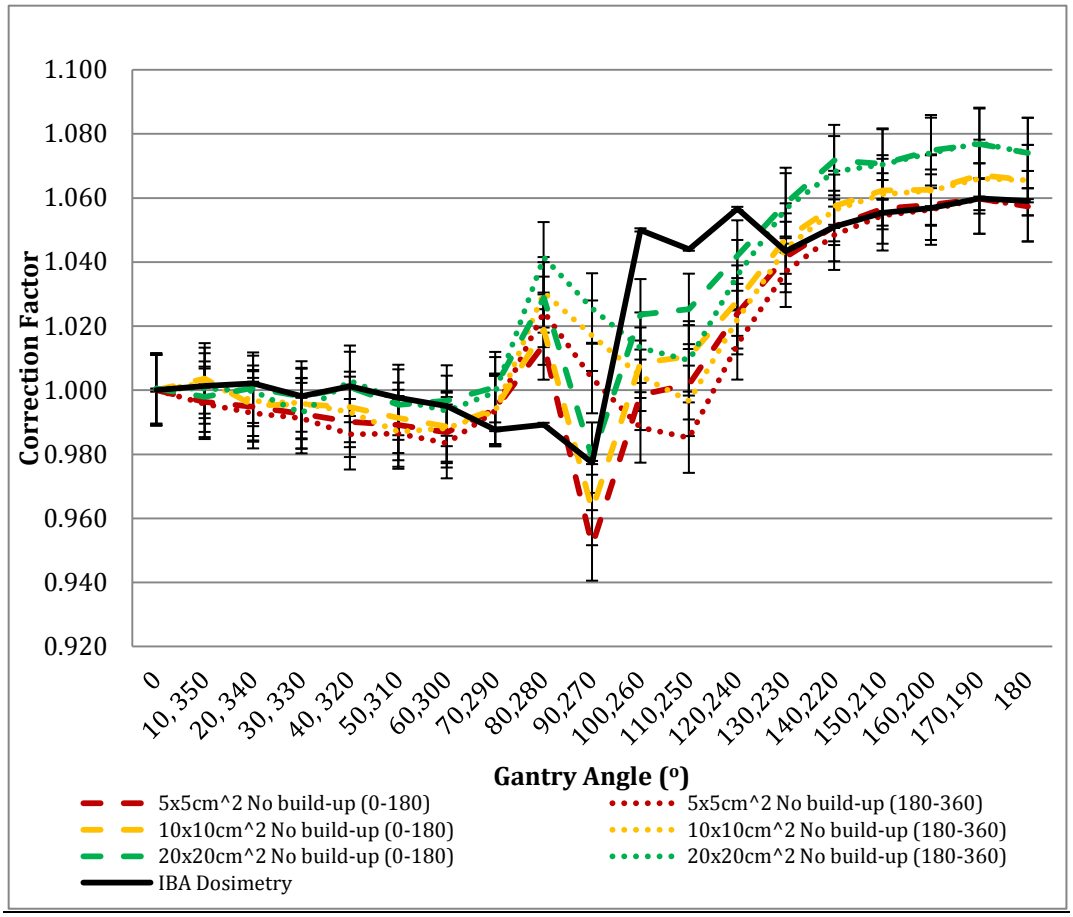

Figure 25: Derived equiangular correction factors without build-up and the IBA Dosimetry correction factors.

Figure 26 plots the equiangular correction factors for 5 x 5 cm^2, 10 x 10 cm^2 and 20 x 20 cm^2 fields with build-up, and the IBA Dosimetry correction factors.

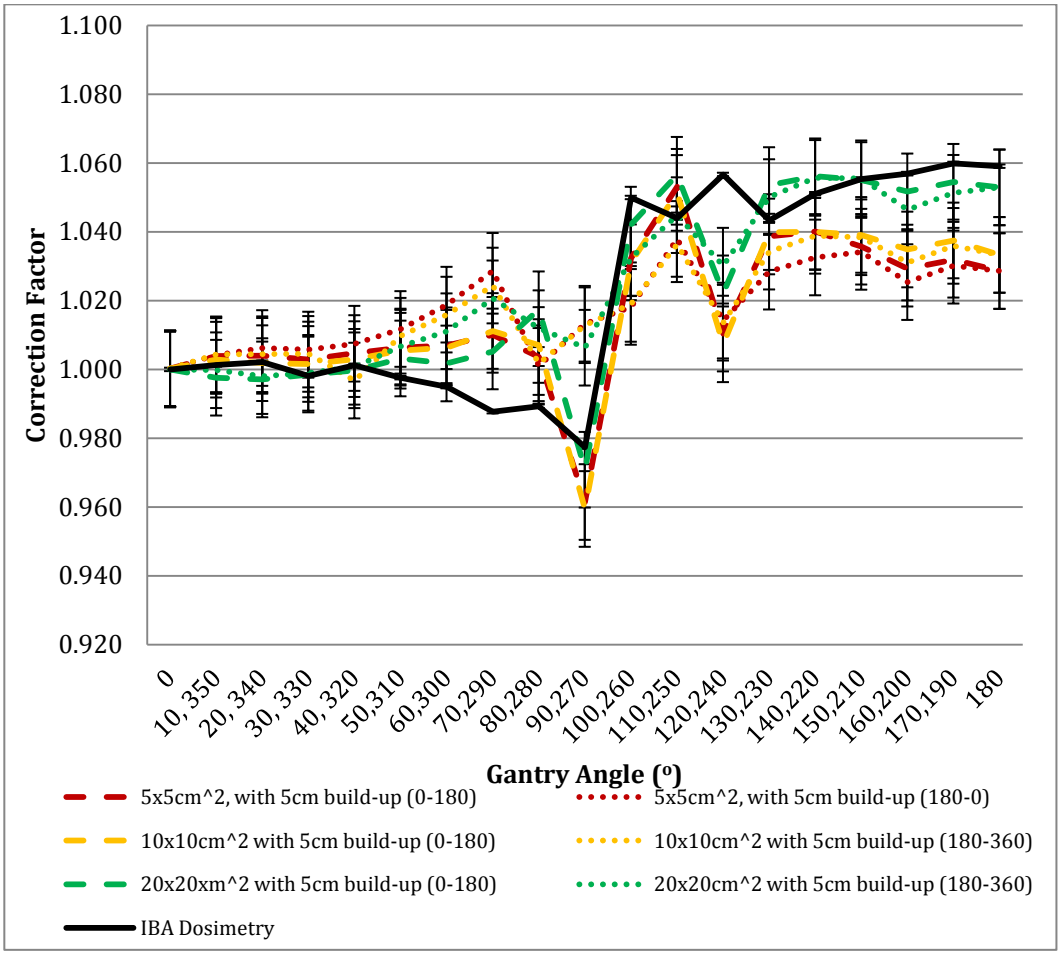

Figure 26: Derived equiangular correction factors without build-up, and the IBA Dosimetry correction factors.

Figures 27 and 28 show the derived correction factors for 5 x 5 cm^2, 10 x 10 cm^2 and 20 x 20 cm^2 fields as a function of gantry angle with and without build-up respectively. The IBA Dosimetry correction factors are also plotted.

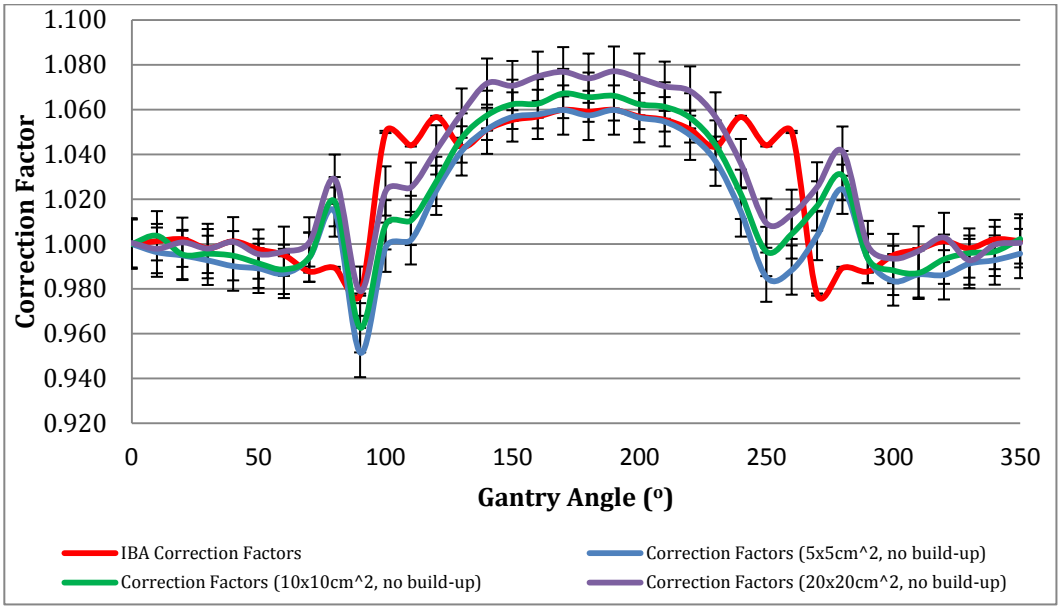

Figure 27: Derived correction factors and IBA Dosimetry correction factors for fields without build-up

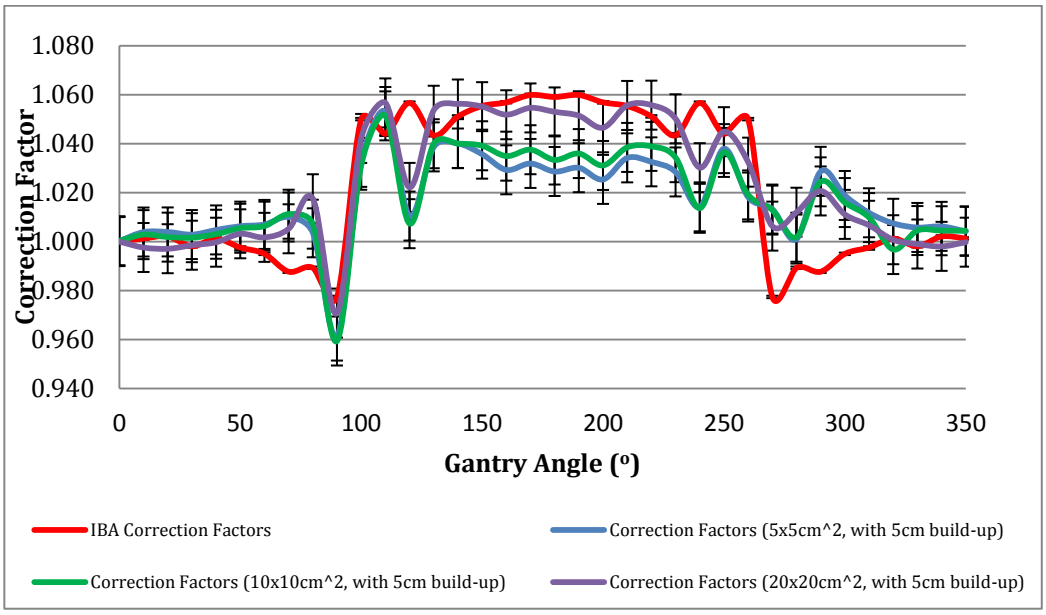

Figure 28: Derived correction factors and IBA Dosimetry correction factors for fields with build-up

5.9. How couch angle affects correction factors

Figure 29 shows the derived correction factors for when the treatment couch is at an angle of 0° and 45°, without build-up, as described in section 4.9. In order to avoid irradiating the electronics of the MatriXX the range of gantry angle was restricted to the angular range from 0° to 180°. The IBA Dosimetry correction factors are also plotted.

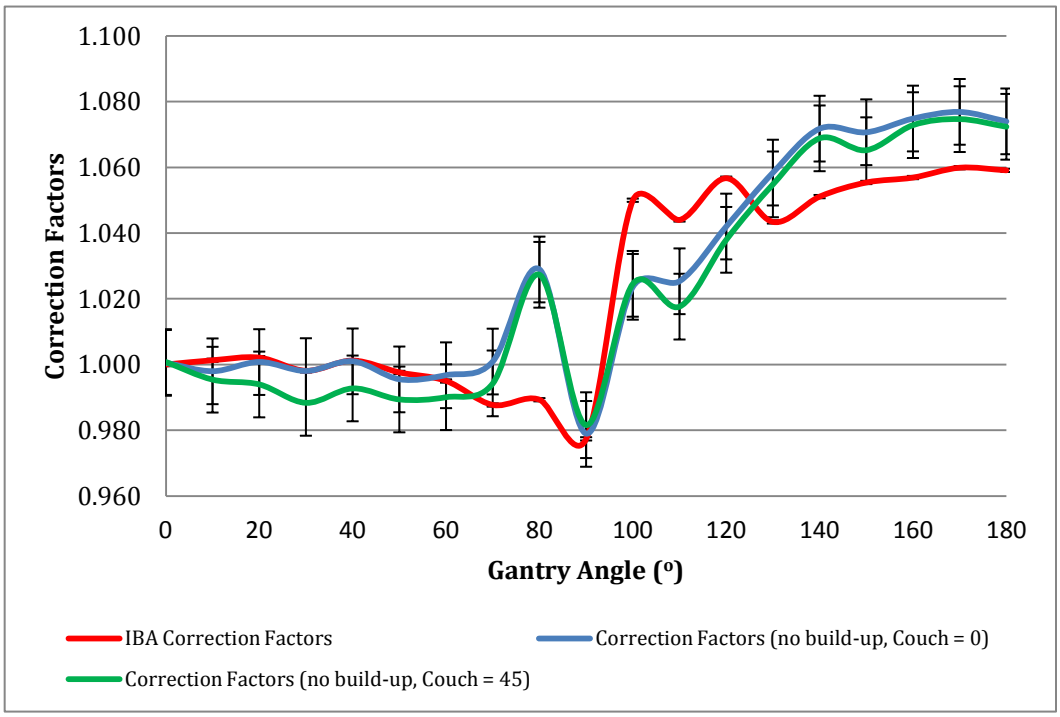

Figure 29: Derived correction factors for when the couch is at 0° and 45° and the MatriXX has no build-up. IBA Dosimetry correction factors are also plotted

Figure 30 shows the derived correction factors with build-up, at couch angles of 0° and 45° for the gantry angles ranging from 0° to 180°. The IBA Dosimetry correction factors are also plotted.

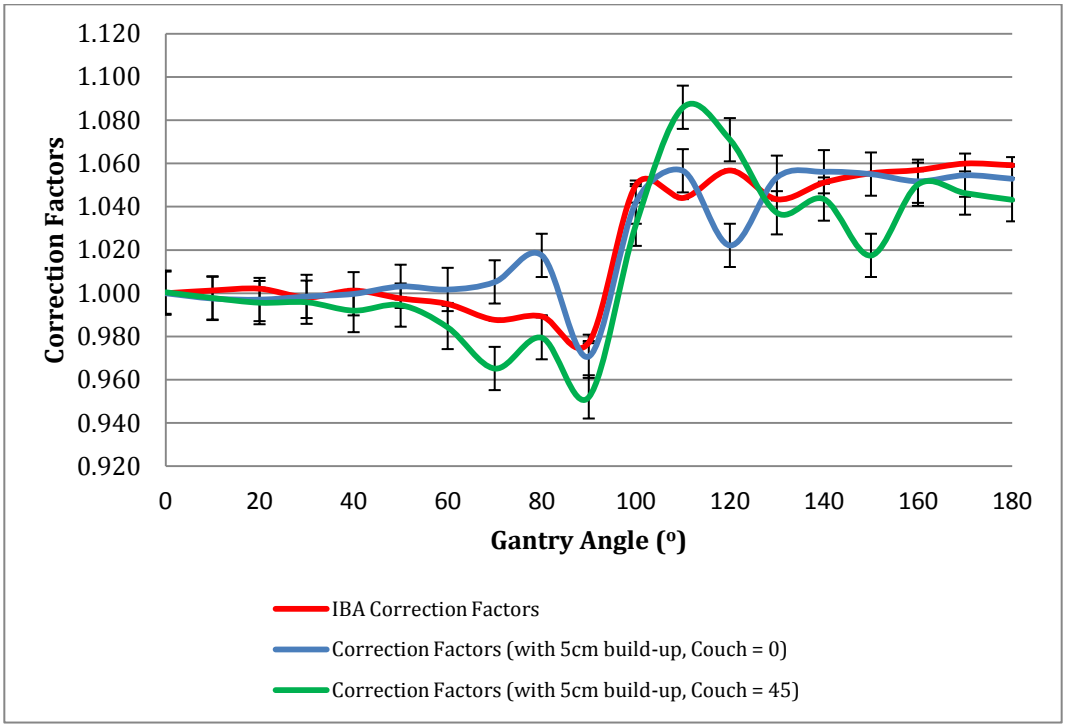

Figure 30: Derived correction factors for when the couch is at 0° and 45° and the MatriXX has 5cm of build-up. IBA Dosimetry correction factors are also plotted

5.10. How intra field position affects correction factors

Figures 31 to 33 show the derived correction factors found at 5 positions within 5 x 5 cm^2, 10 x 10 cm^2 and 20 x 20 cm^2 fields without build-up, in the geometry described in section 4.10.

Figures 34 to Figure 36 show the derived correction factors found at 5 positions within 5 x 5 cm^2, 10 x 10 cm^2 and 20 x 20 cm^2 field with build-up, in the geometry described in section 4.10.

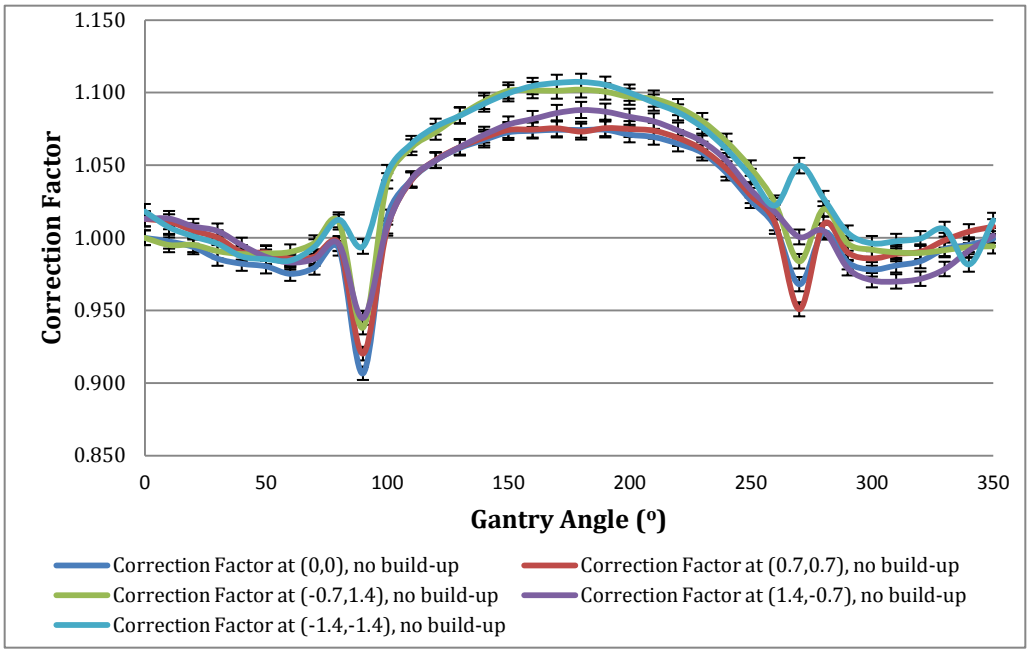

Figure 31: Derived correction factors within a 5x5 cm^2 field without build-up

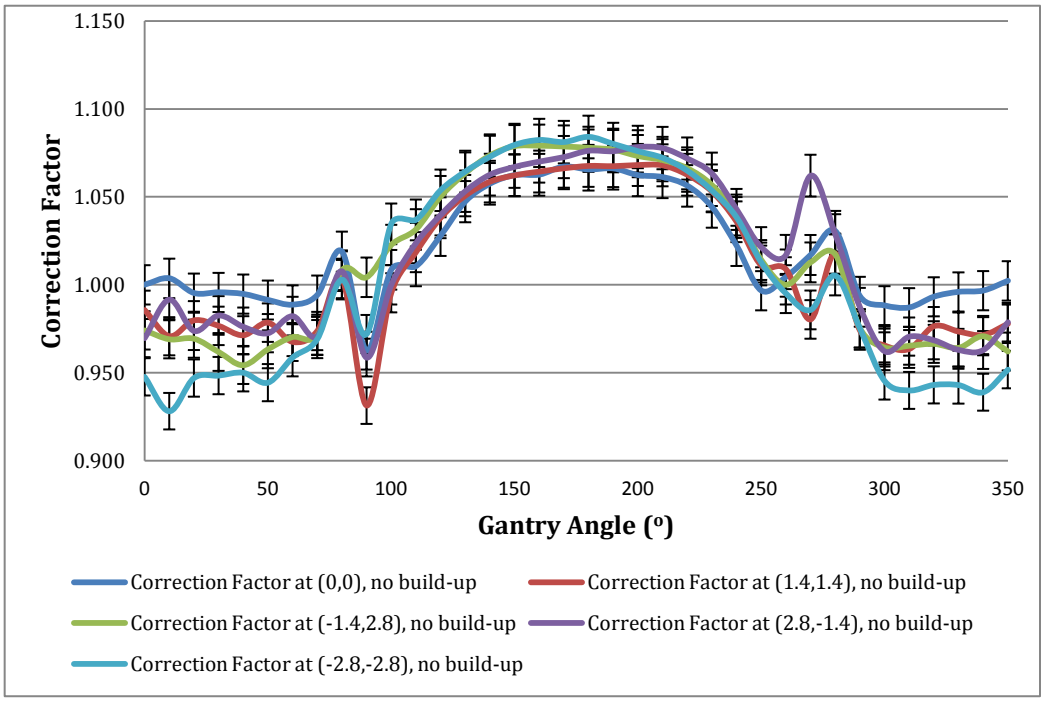

Figure 32: Derived correction factors within a 10x10 cm^2 field without build-up

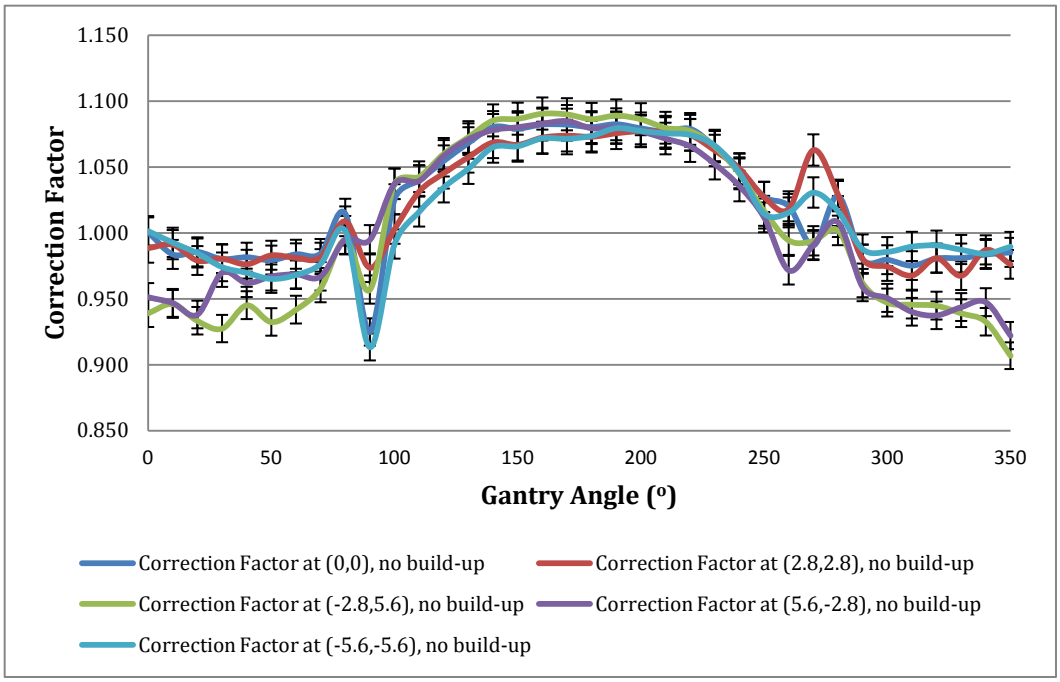

Figure 33: Derived correction factors within a 20x20 cm^2 field without build-up

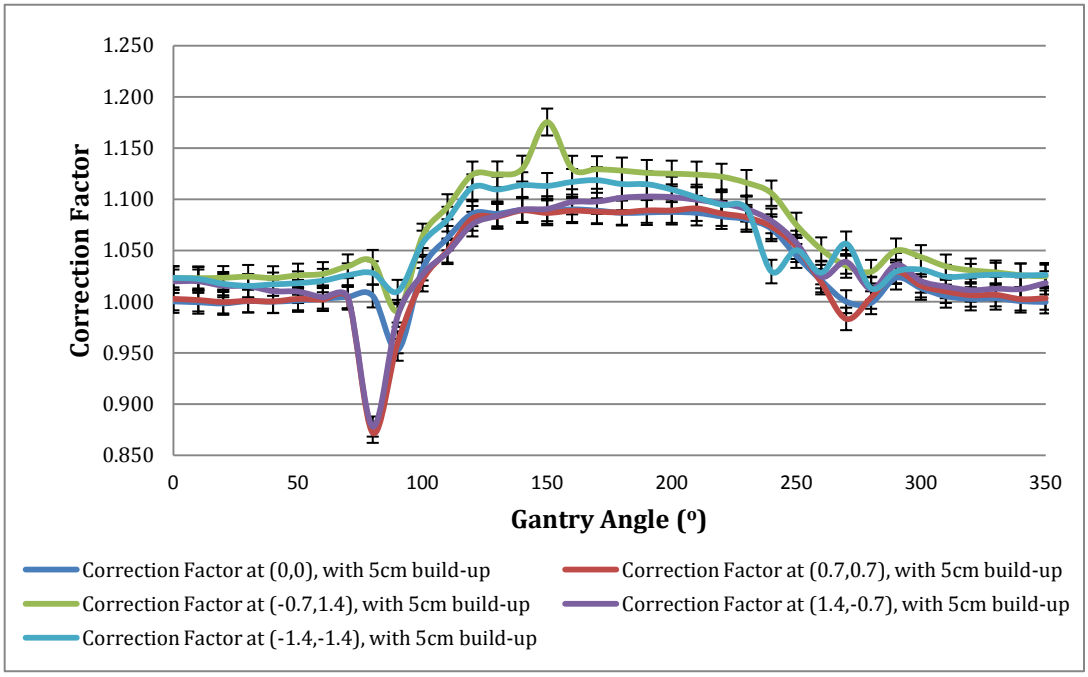

Figure 34: Derived correction factors within a 5x5 cm^2 field with build-up

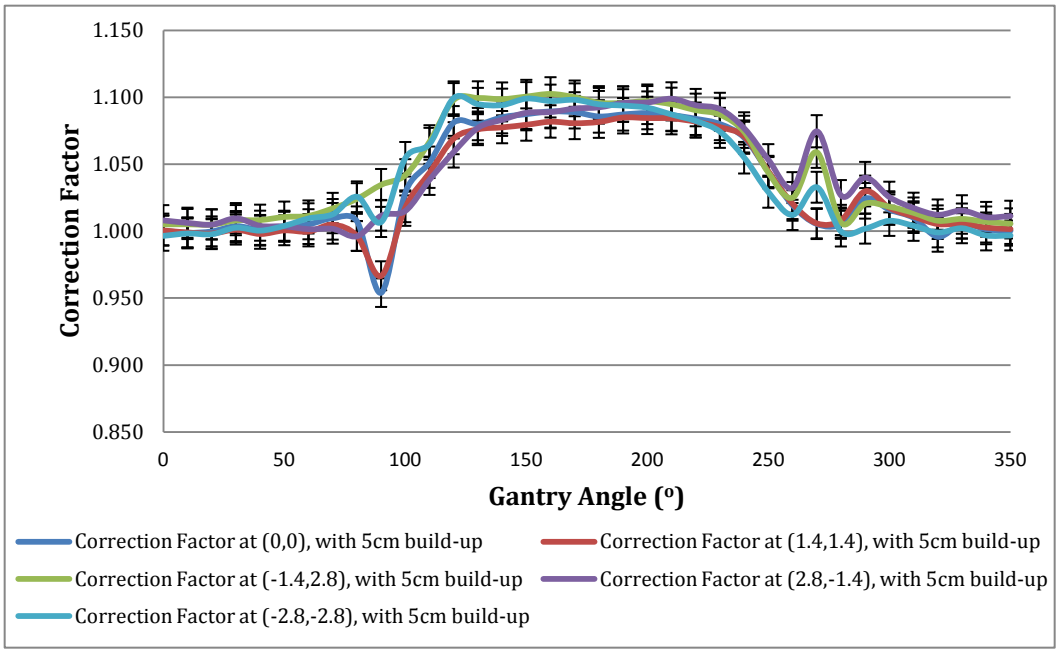

Figure 35: Derived correction factors within a 10x10 cm^2 field with build-up

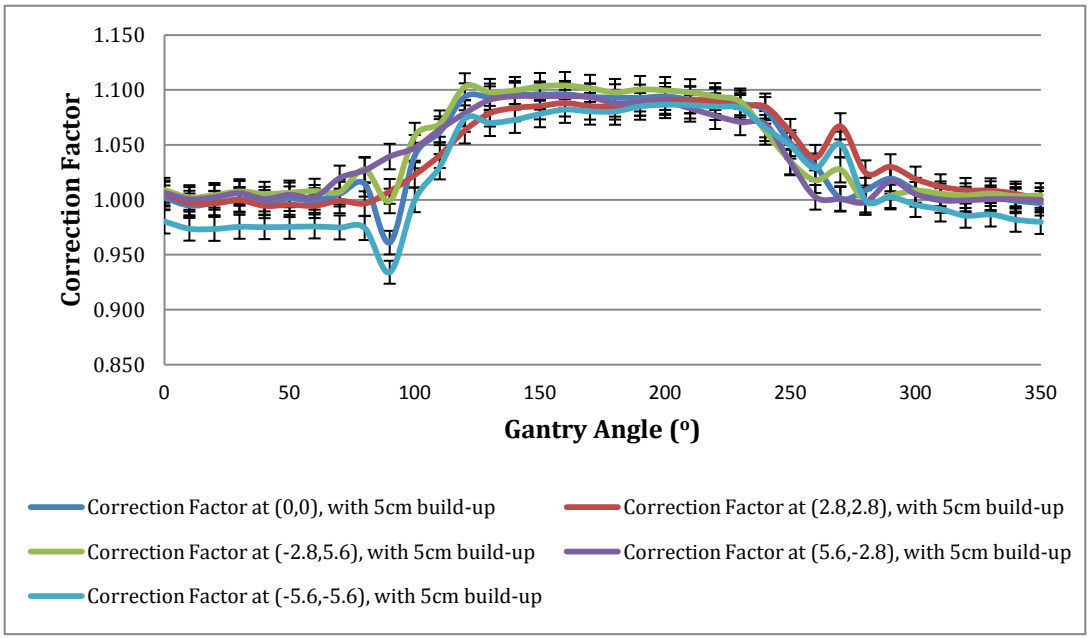

Figure 36: Derived correction factors within a 20x20 cm^2 field with build-up

6. Discussion

6.1. Initial Setup

IMRT and VMAT are two types of treatment that use dynamic Multi Leaf Collimators and a varying dose rate in order to provide radiation treatments which are shaped to provide optimized dose distributions. IMRT may be delivered by the step and shoot method, where beams at several gantry angles are used. VMAT relies on one or more arcs, with varying gantry speed and dose rate. The complexity of these treatments requires patient-specific quality assurance

IBA Dosimetry manufactures a 2-dimensional ion chamber matrix, known as the MatriXX Evolution, as a tool for patient-specific quality assurance. When placed on the Exact® IGRT couch and irradiated at successive gantry angles at 10° increments it was found that the MatriXX dose did not match that calculated by the Philips Pinnacle^{3} TPS. Between the gantry angles of 320° and 40° the absolute differences ranged from 1.2% to 1.5%, with the largest difference being at 0° and 350°. Between the gantry angles of 50° and 130° the absolute difference ranged from 0.4% to 12.2%. The difference was 12.2% at a gantry angle of 110°. Within the gantry angles of 140° to 220° the absolute difference was between 10.0% and 11.2%, with the greatest difference occurring between 150° and 180°. The absolute difference between 230° and 310° ranged from 0.7% to 9.7%. The difference at 230° was 9.7% (Figure 10 and Figure 11). These discrepancies are consistent with those found by Wolfsberger we al. (Wolfsberger, Wagar, Nitsch,

Bhagwat, & Zygmanski, 2010) and are attributed to the anisotropic response of the ion chamber array caused in part by the high Z-air interface at the base of the chambers.

The effective point of measurement was varied within the TPS to determine if the calculated results could match the measured MatriXX dose. At no point within the model of the MatriXX did the TPS calculated dose match the MatriXX measured dose for when the gantry was at 180° (Figure 12). Thus confirms the conclusion of Wolfsberger et al. who also found that the discrepancy cannot be explained by a shift in the effective point of measurement.

Removing the area contoured over the MatriXX ion chambers within the TPS caused a less than 1% difference except between the gantry angles of 80° to 120°, where the greatest difference was 2.2%, at a gantry angle of 100°, and between 250° and 260° where the greatest difference was 1.9%, at a gantry angle of 260° (Figure 13).

6.2. Measuring the dose using an A1SL chamber

Using the A1SL ion chamber to measure the dose and comparing it with the TPS calculated dose gave results that coincided to within 2.2%. The largest dicrepancied occurred when the gantry angles were at 290° and 300°. For the gantry angles between 320° and 40° the differences were under 1% (Figure 14 and Figure 15). This shows that when the point of measurement is moved away from the air-high Z interface the TPS dose corresponding to a posterior geometry

irradiation is in-fact accurate to within about 1% indicating that the discrepancy is due to the anisotropic response MatriXX ion chambers. On the other hand, for laterally directed fields, the TPS dose may be in error by up to 2.2% due to inaccurate accounting for effective path length.

6.3. A comparison of Tissue Phantom Ratios (TPR)

Comparisons were made among the doses determined from RadCalc, the MatriXX, the TPS and an ion chamber and electrometer while the gantry was at an angle of 0° at various amounts of polystyrene depth ranging from1.33 cm to 11.0cm, with the results normalized at 5cm. Beyond the dose build-up region all four systems were in agreement (Figure 16). This shows that there is negligible over-response to spectral softening with depth. This is consistent with previous research (Herzen, et al., 2007).

6.4. Testing the couch model using an ion chamber

The ratio of the doses at gantry angles of 0° and 180° were found using the TPS and also an A1SL ion chamber and electrometer. The ratios were found to be in agreement with the TPS calculated ratio being 1.015 ± 0.007 and the measured ion chamber ratio being 1.013 ± 0.007. This means that the couch model used in the TPS is not the cause of the posterior dose differences (Table 2).

6.5. Investigating up-side down orientated MatriXX response to depth

A comparison was made between the dose calculated by the TPS and that measured by the MatriXX while the gantry was at 0°, with the MatriXX upside down, so that the beam passed through the posterior of the MatriXX, at various depths. This was also done with the gantry at 180° with the beam passing through the couch. In both cases the discrepancy corresponds to a difference of nearly 4 cm of build-up depth. In other words about 4cm additional build-up depth is needed in the TPS model to account for this difference. Alternatively, if the MatriXX is calibrated using posterior irradiation geometry, then the discrepancy is resolved as is evidenced by the good match once the data are re-normalized (Figure 17 and Figure 18).

6.6. Investigating MatriXX response to field size, for different build-ups with the MatriXX oriented right side up and upside down

Comparisons were made between the two systems using 7 different field sizes (1x1cm^2, 2x2cm^2, 5 x 5cm^2, 10 x 10 cm^2, 15x15cm^2, 20 x 20 cm^2 and 25x25cm^2). The comparisons were made at depths of 0.5cm, 3.25cm, 5.0cm and 10.0cm (including intrinsic build-up) and with the MatriXX right side up (Figure 19). The ratio of the TPS dose to MatriXX dose with just intrinsic depth (0.5 cm), for field sizes that are greater than 2x2cm^2, shows a dependence with field size, this may be due to neglect of the field size dependence of electron contamination in the TPS model. The ratio of the TPS dose to the MatriXX dose

at total depths of 3.25 and 5.0 cm were close to unity for field sizes larger then 5x5cm^2, although there was a slight but visible upward trend as field size increased (Figure 20). This has been shown previously (Li, Yan, & Liu, 2009). The ratio of the TPS dose to the MatriXX dose at 10 cm depth does not follow this trend and the ratios do not match results found in Section 8.3, this discrepancy bears further investigation.

Comparisons were made between the two systems at the same field sizes and with a total build-up, including intrinsic build-up, of 3.25cm, 5.0 cm and 10.0cm with the MatriXX upside down. There was discrepancy between the absolute dose of both systems, regardless of field size or build-up (Figure 21).

The ratio of the TPS dose to the MatriXX dose, with the MatriXX upside down, showed a visible upward trend as field size increased. The ratio varied by ± 1% (Figure 22).

6.7. Creating a MatriXX model within the TPS to match the MatriXX results

An attempt was made to create a TPS model that would reproduce the gantry angle dependent response of the MatriXX. Models were created within the TPS, with variously shaped contoured regions overridden with a variety of densities. Two of the models are presented here: the “Foil model” which has a contoured foil placed within the MatriXX image and the “Wedge Model” which has an air wedge within the couch. The results (Figure 23) show that both models

attenuate beams incident from below the MatriXX in order to match the MatriXX response over a gantry range within 20° of directly posterior incidence. However, neither model is capable of compensating beams within about 30° of horizontal incidence. Note that the model compensation is only appropriate for dose to the central pixels. It is not possible to create a single model that will compensate the MatriXX response for all pixels and for any field size or shape.

6.8. Comparing the derived correction factors with those given by IBA Dosimetry

The manufacturer of the MatriXX, IBA Dosimetry, provides correction factors that can be used to correct the dose measured for non-normal incidence. Using the raw MatriXX measurements and corresponding TPS calculated dose, correction factors were derived for the full range of gantry angles and compared to those provided. Correction factors were determined with and without build-up. IBA Dosimetry provides the correction factors for gantry angles of 0° to 80° in increments of 10°, for gantry angles of 86° to 95° in increments of 1° and from 100° to 180° in increments of 10°. Using a field of 20 x 20 cm^2 the derived correction factors and the manufacturer's correction factors were plotted (Figure 24).

With no build-up on the MatriXX the derived correction factors were comparable with those provided to within ± 1% from gantry angles of 0° to 70°. When the gantry angle was 75° and 80° the derived correction factors differed

from the manufacturers by less than absolute difference of 2%. For gantry angles between 85° and 100° the correction factors differed by up to ± 10%, and from 105° to 180° the correction factors differed by less than ± 2%.

With the MatriXX inserted into the "Pelvis Phantom" the two sets of correction factors were comparable to within ±1% for gantry angles of 0° to 60°. For gantry angles of 65° and 70° the correction factors were within ± 2% of each other. Between the gantry angles of 75° to 95° the absolute difference between the two correction factors was less than 9%. With the exception of when the gantry was at 120°, where the difference between the correction factors was ± 3.5%, the difference between the correction factors for gantry angles of 100° to 180° was less than ± 1%.

IBA Dosimetry provides a single set of correction factors for gantry angles from 0° to 180°. For gantry angles ranging from 180° to 360° correction factors are used that correspond to the angle that the gantry makes with the vertical, for example the correction factor for the gantry at 10° is used for the gantry at 350°.

The derived correction factors were symmetric about the vertical, for all six geometries, to within ± 2%, except when at 90° and 270°. At the laterals the difference was as much as ± 6% (Figure 25 and Figure 26).

A single set of correction factors is proposed by the manufacturer regardless of field size and build-up depths. To test the independence of correction factors on field size and build-up depth the measurements were

repeated for three field sizes (5 x 5cm^2, 10 x 10 cm^2 and 20 x 20 cm^2) both with and without build-up (Figure 27 and Figure 28). The results are summarized in table 3.

Table 3: Summary of results comparing derived correction factors with those provided by IBA Dosimetry

Geometry	Gantry Range	% Difference
5x5 cm^2 No Build-up	0°-70°	≤ 2%
	80°-120°	≤ 6%
	130°-230°	≤ 2%
	240°-280°	≤ 6.5%
	290 - 350o	≤ 2.0%
10x10 cm^2 No Build-up	0°-70°	≤ 2%
	80°-120°	≤ 5%
	130°-230°	≤ 1%
	240°-280°	≤ 5%
	290° - 350°	≤ 2%
20x20 cm^2 No Build-up	0°-70°	≤ 2%
	80°-100°	≤ 4%
	110°-230°	≤ 2%
	240°-280°	≤ 5%
	290°-350°	≤ 2%

Geometry	Gantry Range	% Difference
5x5 cm^2 5 cm Build-up	0°-60°	≤ 2%
	70°	2.2%
	80°-120°	≤2%
	120°	4.6%
	130°-230°	≤ 3%
	240°-300°	≤ 5%
	310°-350°	≤ 2%
10x10 cm^2 5 cm Build-up	0°-60°	≤ 2%
	70°	2.3%
	80°-110°	≤ 2%
	120°	≤ 5%
	130° - 230°	≤ 3%
	240°-290°	≤ 4%
	300°	2.1%
	310°-350°	≤ 2%
20x20 cm^2 5 cm Build-up	0°-70°	≤ 2%
	80°	≤ 3%
	90°-110°	≤ 2%
	120°	3.4%
	130°-230°	≤ 1.0%
	240°-290°	≤ 3.5%
	300°-350°	≤ 2%

6.9. How couch angle affects correction factors

Comparing the correction factors derived with the couch is at 0° with those derived with the couch at 45° shows that the correction factors match well without build-up but less so with build-up (Figure 29 and Figure 30). The maximum

discrepancy for the MatriXX without build-up was ± 1%, at a gantry angle of 30°. When the MatriXX had build-up the absolute difference was less than 2% for a gantry range of 0° to 60°. When the gantry angle was 70° and 80° the absolute difference was less 4%. For 90° and 100° gantry angles, the difference was ± 2%. For gantry angles of 110° to 150° the absolute difference was less than 5%. For gantry angles of 160° to 180° the difference was less than ± 1%.

6.10. How intra field position affects correction factors

The correction factors were derived at five different positions: one at the central axis position and the other four placed in each quadrant, for three different field sizes (5 x 5cm^2, 10 x 10 cm^2 and 20 x 20 cm^2), both with and without build-up (Figure 31 to Figure 35). The results are summarized in Table 4 and 5.

Table 4 reports the maximum percentage difference between the derived correction factors at the centre position and at each quadrant point, along with the gantry angle corresponding to the maximum percentage difference. Table 5 shows the maximum percentage difference between correction factors found at the centre position and those at the quadrant point corresponding to the maximum percentage difference over specific gantry angle ranges.

Table 4: Summary of results for within field correction factors; maximum percentage difference within at each measurement position

Geometry	Position	Max. % Diff	Gantry Angle
5x5 cm^2 No Build-up	(0.7,0.7)	1.8	270°
	(-0.7,1.4)	3.5	90°
	(-1.4,0.7)	4.2	90°
	(-1.4,-1.4)	9.6	90°
10x10 cm^2 No Build-up	(1.4,1.4)	3.6	270°
	(-1.4,2.8)	4.3	90°
	(-2.8,1.4)	4.4	270°
	(-2.8,-2.8)	7.5	10°
20x20 cm^2 No Build-up	(2.8,2.8)	7.3	270°
	(-2.8,5.6)	8.0	350°
	(-5.6,2.8)	7.6	90°
	(-5.6,-5.6)	4.1	270°
5x5 cm^2 5cm Build-up	(0.7,0.7)	13.3	80°
	(-0.7,1.4)	8.0	150°
	(-1.4,0.7)	12.7	80°
	(-1.4,-1.4)	6.0	90°
10x10 cm^2 5cm Build-up	(1.4,1.4)	1.3	90°
	(-1.4,2.8)	8.5	90°
	(-2.8,1.4)	6.9	270°
	(-2.8,-2.8)	5.5	90°
20x20 cm^2 5cm Build-up	(2.8,2.8)	6.6	270°
	(-2.8,5.6)	3.9	90°
	(-5.6,2.8)	8.2	90°
	(-5.6,-5.6)	4.9	270°

Table 5: Summary of results for within field correction factors; maximum percentage difference within gantry ranges

Gantry Range	Depth	Max % Difference	Field-Size	Position
320°-40°	No build-up	8.0%	20x20cm^2	-2.8,5.6
50°-130°	No build-up	9.6%	5x5cm^2	-1.4,-1.4
140°-220°	No build-up	3.0%	5x5cm^2	-1.4,-1.4
230°-310°	No build-up	8.4%	5x5cm^2	-1.4,-1.4
320°-40°	Build-up	2.8%	5x5cm^2	-0.7,1.4
50°-130°	Build-up	13.3%	5x5cm^2	0.7,0.7
140°-220°	Build-up	8.0%	5x5cm^2	-0.7,1.4
230°-310°	Build-up	6.9%	10x10cm^2	2.8,-1.4

7. Conclusion

The MatriXX Evolution, a 2-dimensional ion chamber array, is used for patient-specific quality assurance measurements of IMRT and VMAT radiotherapy at the JCC. These treatments rely on gantry rotation, either in the "step-and-shoot" of IMRT or using arcs as is done in VMAT. MatriXX measurements were found to not match calculated doses values, particularly for beams incident on the posterior side of the MatriXX. This discrepancy is not a result of the couch model used in the TPS, nor is it due to the TPS model. The discrepancy is attributed to a strong directional dependence of the MatriXX ion chamber response.

An attempt to model the directional dependence of the ion chamber response empirically within the TPS was partially successful as long as irradiation was restricted to within 60° of normal incidence from the anterior or posterior side of the MatriXX.

IBA Dosimetry has supplied a set of gantry angle dependent correction factors. In this work, MatriXX measurements over a broad range of irradiation geometries have been performed and compared to TPS calculation to evaluate the suitability of this set. The supplied correction factors were compared with factors derived from the MatriXX measurements and TPS calculations. It was found that the supplied and the derived correction factors generally agreed except between the gantry angles of 75° to 100°. The greatest discrepancy occurred for the 5 x 5

cm^2 field without build-up at a gantry angle of 260° (5.9%). The geometry that had the lowest maximum error over the full range of gantry angles was the 20 x 20 cm^2 fields (3.3%), when the MatriXX was held in the "Pelvis Phantom". The greatest difference for the 10 x 10 cm^2 field without build-up was at the gantry angle of 250° (4.5%). The greatest difference for the 10 x 10 cm^2 fields with build-up was at the gantry angle of 120° (4.7%). This is summarized in Table 3.

Each MatriXX set-up had a range of anterior gantry angles where the discrepancy between the derived correction factors and those produced by the manufacturer were in agreement within 1%. For the 5 x 5 cm^2 field without build-up the range was 330° to 30°. For the 5 x 5 cm^2 field with build-up the range was 320° to 50°. For 10 x 10 cm^2 field without build-up the range was 310° to 70°. For the 10 x 10 cm^2 field with build-up the range was 320° to 50°. For the 20 x 20 cm^2 field without build-up the range was 300° to 60°. For the 20 x 20 cm^2 field with build-up the range was 310° to 60°. This is shown in Table 5.

The large calculated variation in lateral correction factors with small changes in gantry angle suggest that these correction factors should be sampled on a finer angular grid. Since the MatriXX response to left and right lateral fields were found to not be symmetric, separate correction factors should be used for right and left laterally directed fields.

The difference between the correction factors at gantry angles of 90° and 270° occurs due to the directional dependence of the MatriXX ion chambers. In future correction factors should be measured for fields of similar size and delivered by the same technique (IMRT or VMAT) as those being verified. Measurements should be made using the same irradiation geometry (i.e MatriXX within the "Pelvis Phantom") as used for clinical QA. These considerations ensure that the MatriXX is irradiated with a spectrum of photons representative of those delivered clinically. This spectrum is influenced by MLC transmission and depth of the ion chamber array within the phantom. Spectral effects on the <atriXX response have not been directly investigated here, but their magnitude may be inferred from the results above. A previous study has shown that with the appropriate correction factors applied, good agreement can be achieved (Han, Ng, Bhagwat, Lyatskaya, & Zygmanski, 2010). Within field correction factors show some large discrepancies, particularly at the lateral positions.

Another way to eliminate the problem of directional dependence of the MatriXX ion chambers is to mount the measurement device on a rigid structure attached to the gantry head. The mounting device is available commercially or made in-house. The mount required testing and maintenances that there is no shift or sag during gantry rotation. The drawback of this using this approach is that it does not reflect the dose distribution delivered to the patient and is therefore of limited clinical interest.

References

Almond, P. R., Biggs, P. J., Coursey, B. M., Hanson, W. F., Huq, M. S., Nath, R., et al. (1999). AAPM's TG-51 protocol for clinical reference dosimetry of high-energy photon and electron beams. *Medical Physics , 26* (9), 1847-1870.

Amerio, S., Boriano, A., Bourhaleb, F., Cirio, R., Donetti, M., Fidanzio, A., et al. (2004). Dosimetric charcterization of a large area pixel-segmented ionization chamber. *Medical Physics , 31* (2), 414-420.

Bjoern Poppe, A. B. (2006). Two-dimensional ionization chamber arrays for IMRT plan verification. *Medical Physics , 33* (4), 1005-1015.

Bortfeld, T. (1999). Optimized Planning Using Physical Criteria. *Seminars in Radiation Oncology , 9* (1), 20-34.

Bortfeld, T. (2010). The number of beams in IMRT- theoretical investigations and implications for single-arc IMRT. *Physics in Medicine and Biology , 55*, 83-97.

Buckey, C. R., Stathakis, S., & Papanikolaou, M. (2010). The inter- and intrafraction reproducibilities of three common IMRT delivery techniquies. *Medical Physics , 37* (9), 4854-4860.

Burman, C., Chui, C., Kutcher, G., Leibel, S., Zelefsky, M., LoSasso, T., et al. (1997). Planning, delivery, and quality assurance of intensity-modulated radiotherapy using dynamic multileaf collimator: A strategy for large-scale implementation for the treatment of carcinoma of the prostate. *International Journal of Radiation Oncology Biology Physics , 39* (4), 863-873.

Bzdusek, K., Friberger, H., Eriksson, K., Hårdemark, B., Robinson, D., & Kaus, N. (2009). Devolopment and evaluation of an efficient approach to volumetric arc therapy planning. *Medical Physics , 36* (6), 2328-2339.

Currell, G., & Dowman, A. (2009). Essential Mathematics and Statistics for Science. In G. Currell, & A. Dowman, *Essential Mathematics and Statistics for Science* (2nd Edition ed.). Hoboken: John Wiley & Sons, Ltd.

E. Spezi, A. L. (2005). Characterization of a 2D ion chamber array for the verification of radiotherapy treatments. *Physics in Medicine and Biology , 50*, 3361-3373.

FlukeCorporation. (2012). *35040*. (Fluke Corporation) Retrieved August 03, 2012 from Fluke Biomedical: http://www.flukebiomedical.com/biomedical/usen/Radiation-Oncology-QA/Linear-Accelerator-QA/35040.htm?PID=54666

Han, Z., Ng, S. K., Bhagwat, M. S., Lyatskaya, Y., & Zygmanski, P. (2010). Evaluation of MatriXX for IMRT and VMAT dose verifications in peripheral dose regions. *Medical Physics , 37* (7), 3704-3714.

Herzen, J., Todorovic, M., Cremers, F., Platz, V., Albers, D., Bartels, A., et al. (2007). Dosimetric evaluation of a 2D pixel ionization chamber for implementation in clinical routine. *Physics in Medicine and Biology , 52*, 1197-1208.

Hope, C. S., Laurie, J., & Hanlan, K. E. (1967). Optimization of X-ray Treatment Planning b y Computer Judgement. *Physics in Medicine and Biology , 12* (4), 531-542.

IBA Dosimetry. (2012). *http://www.iba-dosimetry.com/sites/default/files/brochure/MatriXX-Evolution_01.pdf*. (iba Dosimetry) Retrieved August 03, 2012 from IBA Dosimetry: http://www.iba-dosimetry.com/sites/default/files/brochure/MatriXX-Evolution_01.pdf

IBA Dosimetry. (2012). *MAtriXX Detectors | Dosimetry*. (iba) Retrieved August 03, 2012 from iba Dosimetry Web Site: http://www.iba-dosimetry.com/complete-solutions/radiotherapy/imrt-igrt-rotational-qa/matrixxes

Koninklijke Philips Electronics N.V. (2012). *Pinnacle3 - Philips*. (Koninklijke Philips Electronics N.V.) Retrieved August 03, 2012 from Philips web site: http://www.healthcare.philips.com/ca_en/products/ros/products/pinnacle3

Korevaar, E. W., Wauben, D. J., Hulst, P. C., Langendijk, J. A., & Veld, A. A. (2011). Clinical introduction of a linac head-mounted 2-D detector array based quality assurance system in head and neck IMRT. *Radiotherapy and Oncology , 100*, 446-452.

Li, J. G., Yan, G., & Liu, C. (2009). Comparison of two commercial arrays for IMRT quality assurance. *Journal of Applied Clinical Medical Physics , 10* (2), 62-74.

Ling, C. C., Zhang, P., Archambault, Y., Bocanek, J., Tang, G., & LoSasso, T. (2008). Commissioning and quality assurance of Rapidarc radiotherapy delivery system. *International Journalof Radiation Oncology Biology Physics , 72* (2), 575-581.

M. Stasi, S. G. (2005). D-IMRT verification with a 2D pixel ionization chamber: dosimetric and clinical results in head and neck cancer. *Physics in Medicine and Biology , 50*, 4681-4693.

Mihaylov, I., Bzdusek, K., & Klaus, M. (2011). Carbon fiber couch effects on skin dose for volumetric modulated arcs. *Medical Physics , 38* (5), 2419-2423.

OmniPro-I'mRT Software. (2012). Retrieved Sep 07, 2012 from iba Dosimetry: http://www.iba-dosimetry.com/complete-solutions/radiotherapy/imrt-igrt-rotational-qa/omnipro-i-mrt

Otto, K. (2008). Volumetric modulated arc therapy: IMRT in a single gantry arc. *Medical Physics , 35* (1), 310-317.

Schreibmann, E., Dhabaan, A., Elder, E., & Fox, T. (2009). Patient-specific quality assurance method for VMAT treatment delivery. *Medical Physics , 36* (10), 4530-4535.

Shepard, D. M., Cao, D., Afghan, M. K., & Earl, M. A. (2007). An arc sequencing algorithm for intensity modulated arc therapy. *Medical Physics , 34* (2), 464-470.

Shimohigasi, Y., Araki, F., Tominaga, H., Sakata, J., Kawasaki, K., Kanetake, N., et al. (2012). Angular dependence correction of MAtriXX and its application to composite dose verification. *Journal of Applied Clinical Medical Physics , 13* (5), 198-214.

Standard Imaging Inc. (2012). *Exaradin A1SL Ion Chamber - Product Home*. (Dynamsoft SourceAnywhere) Retrieved August 03, 2012 from Standard Imaging Inc web site: http://www.standardimaging.com/product_home.php?id=26

Standard Imaging, Inc. (2012). *Stereotactic Dose Verification Phantom*. (Dynamsoft SourceAnywhere) Retrieved August 03, 2012 from Standard Imaging Inc web site: http://www.standardimaging.com/product_home.php?id=63

Sun Nuclear Corporation. (2012). *Sun Nuclear - Your most valuable QA and dosimetry tools*. Retrieved Sep 05, 2012 from Un Nuclear Corporation: http://www.sunnuclear.com/medphys/patientqa/radcalc/radcalc.asp

Tang, G., Earl, M. A., & Yu, C. X. (2009). Variable dose rate single-arc IMAT delivered with a constant dose rate and variable angular spacing. *Physics in Medicine and Biology , 54*, 6439-6456.

Vanetti, E., Nicolini, G., Clivio, A., Fogliata, A., & Cozzi, L. (2009). The impact of treatment couch modelling on Rapidarc. *Physics in Medicine and Biology , 54*, N157-N166.

Varian Medical Systems Inc. (2012). *Exact IGRT Couch and Indexed Immobilization (Optional)*. (Varian Medical Systems Inc) Retrieved August 03, 2012 from Varian Medical Systems Inc: http://www.varian.com/us/oncology/radiation_oncology/clinac/exact_igrt_couch.html

Varian Medical Systems Inc. (2012). *Linear Accelerator | Trilogy Delivery System*. (Varian Medical Systems Inc) Retrieved August 03, 2012 from Varian Medical Systems Corporation Web site: http://www.varian.com/us/oncology/radiation_oncology/trilogy/

Webb, S., & McQuaid, D. (2009). Some considerations concerning volume-modulated arc therapy: a stepping stone towards a general theory. *Physics in Medicine and Biology , 54*, 4345-4360.

Wolfsberger, L. D., Wagar, M., Nitsch, P., Bhagwat, M. S., & Zygmanski, P. (2010). Angular dose dependency of MatriXX TM and its calibration. *Journal of Applied Clinical Medical Phsyics* , *11* (1), 241-251.

Yu, C. X. (1995). Intensity modulated arc therapy with dynamic multileaf collimation: an alternative to tomotherapy. *Physics in Medicine and Biology* , *40*, 1435-49.